

# Mutations in the Substrate Binding Domain of the *Escherichia coli* 70 kDa Molecular Chaperone, DnaK, which Alter Substrate Affinity or Interdomain Coupling

Diana L. Montgomery<sup>1</sup>, Richard I. Morimoto<sup>2</sup> and Lila M. Gierasch<sup>1\*</sup>

<sup>1</sup>Department of Chemistry  
University of Massachusetts  
Amherst, MA 01003, USA

<sup>2</sup>Department of Biochemistry  
Molecular Biology, and Cell  
Biology, Northwestern  
University, 2153 North  
Campus Drive, Evanston  
Illinois, 60208, USA

In *Escherichia coli*, DnaK is essential for the replication of bacteriophage  $\lambda$  DNA; this *in vivo* activity provides the basis of a screen for mutations affecting DnaK function. Mn PCR was used to introduce mutations into residues 405–468 of the C-terminal polypeptide-binding domain of DnaK. These mutant proteins were screened for the ability to propagate bacteriophage  $\lambda$  in the background of a *dnaK* deficient cell line, BB1553. This initial screen identified several proteins which were mutant at multiple positions. The multiple mutants were further dissected into single mutants which remained negative for  $\lambda$  propagation. Four of these single-site mutants were purified and assayed for biochemical functionality. Two single-site mutations, F426S and S427P, are localized in the peptide binding site and display weakened peptide binding affinity. This indicates that the crystallographically determined peptide binding site is also critical for *in vivo*  $\lambda$  replication. Two other mutations, K414I and N451K, are located at the edge of the  $\beta$ -sandwich domain near  $\alpha$ -helix A. The K414I mutant binds peptide moderately well, yet displays defects in allosteric functions, including peptide-stimulated ATPase activity, ATP-induced changes in tryptophan fluorescence, ATP-induced peptide release, and elevated ATPase activity. The K414 position is close in tertiary structure to the linker region to the ATPase domain and reflects a specific area of the peptide-binding domain which is necessary for interdomain coupling. The mutant N451K displays defects in both peptide binding and allosteric interaction.

© 1999 Academic Press

\*Corresponding author

Keywords: allosterism; calorimetry; chaperones; DnaK; fluorescence

## Introduction

DnaK is a member of the 70 kDa heat shock protein family (hsp70s). Heat shock proteins derive their name from their high level of selective expression in response to elevated temperature and other forms of cellular stress. After hsp synthesis has reached a significant level, these proteins enhance cellular viability following exposure to high growth temperatures. hsp70s are also expressed constitutively under normal growth conditions where they perform key functions in the cell, e.g. binding to nascent polypeptide chains to maintain solubility, membrane translocation of pre-

cursor proteins, disassembly of specific macromolecular complexes such as clathrin-coated vesicles and  $\lambda$  DNA origin of replication, protein degradation, and modulation of heat shock gene expression (Beckmann *et al.*, 1990; Nelson *et al.*, 1992; Kang *et al.*, 1990; Chappell *et al.*, 1986; Georgopoulos *et al.*, 1990; Straus *et al.*, 1988; Tilly *et al.*, 1983). The functional relationship between these activities and the role of hsp70s during heat shock is thought to be that they bind to unfolded proteins and prevent non-productive folding interactions or aggregation (Pelham, 1986). The activity of preventing irreversible off-pathway folding events has given hsp70 proteins their second name of molecular chaperones. Furthermore, hsp70 proteins have been directly shown to assist the refolding of polypeptide substrates *in vitro*, in the presence of ATP and co-chaperone proteins (Langer *et al.*, 1992; Schröder *et al.*, 1993; Szabo

Abbreviations used: hsp70s, 70 kDa heat shock protein family; wt, wild-type; ; 5-IAF, 5-iodoacetamidofluorescein.

E-mail address of the corresponding author: gierasch@chem.umass.edu

*et al.*, 1994; Freeman *et al.*, 1995; Freeman & Morimoto, 1996).

In *Escherichia coli*, one of DnaK's earliest identified functions came to light as a result of genetic studies of bacteriophage  $\lambda$  DNA replication (for a review, see Georgopoulos *et al.*, 1990). This work indicated that three heat shock proteins (DnaK, DnaJ, and GrpE) were among the *E. coli* host proteins required for  $\lambda$  propagation. Mutation of any one of these three genes resulted in a similar bacterial phenotype, suggesting that these three proteins work in concert. *In vitro* studies of the initiation of bacteriophage  $\lambda$  DNA replication have provided insights to the specific roles of DnaK, DnaJ, and GrpE in this process (Mensa-Wilmot *et al.*, 1989; Zyllicz *et al.*, 1989). At the beginning of the DNA replication process a  $\lambda$  protein ( $\lambda$ O) binds to the  $\lambda$  DNA origin of replication *ori*  $\lambda$ . Another  $\lambda$  protein,  $\lambda$ P, binds to the *E. coli* DNA helicase (DnaB), inactivates it, and localizes it to the  $\lambda$ O-*ori*  $\lambda$  DNA protein complex. In the presence of DnaK, DnaJ, GrpE, and ATP, the *ori*  $\lambda$  macromolecular complex is disrupted, releasing active helicase (DnaB), which can then initiate  $\lambda$  DNA replication (Liberek *et al.*, 1988; Alfano & McMacken, 1989a,b; Dodson *et al.*, 1989).

Biochemical studies with purified proteins showed that DnaJ and GrpE have the capacity to regulate certain enzymatic activities of DnaK, including: (1) DnaJ-dependent enhancement of the rate of ATP hydrolysis by DnaK (Liberek *et al.*, 1991a); (2) GrpE-dependent enhancement of the rate of nucleotide dissociation from DnaK (Liberek *et al.*, 1991a); and (3) DnaJ-dependent stabilization of DnaK-substrate interactions in the presence of ATP (McCarty *et al.*, 1995; Wawrzynów *et al.*, 1995). Because DnaJ and GrpE modulate the activity of DnaK, they are referred to as co-chaperone proteins. Eukaryotic co-chaperone homologs of DnaJ and GrpE have been identified and shown to interact with hsp70 proteins (for reviews, see Hartl, 1996; Brodsky, 1996); hence, DnaK, DnaJ, and GrpE can all be considered to be members of the functional hsp70 molecular chaperone system.

DnaK and hsp70s in general contain two well-characterized functional domains. The N-terminal 45 kDa domain displays ATP hydrolysis activity (Chappell *et al.*, 1987). The atomic structure of this domain has been solved by X-ray crystallography (Flaherty *et al.*, 1990; Harrison *et al.*, 1997). The C-terminal domain corresponds to the remaining 25 kDa, and is responsible for polypeptide substrate binding (Chappell *et al.*, 1987; Milarski & Morimoto, 1989; Wang *et al.*, 1993; Gragerov *et al.*, 1994). In DnaK, polypeptide binding activity remains after truncation of 100 amino acid residues from the C terminus (residues; 1-538; Buchberger *et al.*, 1995). There are currently two structures of fragments of the C-terminal domain of DnaK; one determined by X-ray crystallography (Zhu *et al.*, 1996) and one determined by NMR (Wang *et al.*, 1998). The 2.0 Å resolution structure determined by crystallography contains residues 389-607 of

DnaK in complex with peptide (NRLLLTG). The polypeptide substrate binding domain contains a  $\beta$ -sandwich sub-domain followed by an  $\alpha$ -helical sub-domain. The peptide is bound in an extended conformation between two loops in the  $\beta$ -sandwich sub-domain. The protein forms hydrogen bonds with the backbone of the peptide and a deep hydrophobic pocket which accommodates the central leucine (L<sub>4</sub>) of the peptide.

The two functional domains of hsp70s play a role in the allosteric behavior of the full-length protein; the binding of a ligand to one domain regulates the activity of the other domain. For instance, the binding of ATP lowers the affinity for unfolded substrate polypeptides (Flynn *et al.*, 1989; Liberek *et al.*, 1991b; Schmid *et al.*, 1994). Likewise, the binding of polypeptide substrates can stimulate ATP hydrolysis (Flynn *et al.*, 1989; Braell *et al.*, 1984; Sadis & Hightower, 1992).

One of the most pressing questions in the hsp70 field is how polypeptide substrates are selected (Rüdiger *et al.*, 1997b). Knowledge of the structural and thermodynamic factors that govern substrate binding may lead to the prediction of substrate-hsp70 interactions or the targeting of hsp70 to disruption of specific macromolecular complexes. A second critical question regards the molecular mechanism of interdomain coupling and regulation. We have taken a mutagenesis approach to these issues and specifically targeted amino acid residues within the peptide binding domain. The bacteriophage  $\lambda$  propagation assay was used to screen for the *in vivo* activity of each mutant. There are several advantages of this approach: (1) the screen can be performed in the context of the full-length DnaK protein; (2) the screen uses the highly characterized bacteriophage  $\lambda$  assay which has been studied at both a genetic and biochemical level; and (3) the screen could potentially identify several different biochemical phenotypes, such as defects in polypeptide substrate binding, interdomain coupling, and interactions with co-chaperone proteins. Indeed, the most striking mutant identified in this study, K414I, introduces a defect in interdomain coupling which may not have been identified if a structural-based inspection approach had been used.

## Results

### Production and screening of DnaK mutants

Mutations in the C-terminal peptide binding domain of DnaK were produced by Mn PCR random mutagenesis (Cadwell & Joyce, 1994) of a DNA fragment defined by boundaries of the unique restriction sites of *Nco*I and *Sph*I (between bp 1214-1402) and reinserted into the wild-type (wt) *dnaK* gene at these respective sites. This region, corresponding to amino acid residues 405 to 468 of DnaK, was selected because it corresponds to residues within a suggested minimal peptide binding domain (386-538; Chappell *et al.*,

**Table 1.**  $\lambda$  Propagation activity of DnaK mutants

	0 $\mu$ M IPTG	50 $\mu$ M IPTG
wt	++ <sup>a</sup>	++
K414I, Q424R, K446R	-	+
K414I	- <sup>a</sup>	+/-
K446R	++	n.d.
F426S, Q456R	-	+
F426S	- <sup>a</sup>	+
Q456R	++	n.d.
S427P, N458S, K452R	-	-
S427P	- <sup>a</sup>	-
N458S, K452R	++	n.d.
N451 K	- <sup>a</sup>	+
Vector only	-	-

n.d. = not determined; ++, 1460( $\pm$ 570) plaques; +, <50 plaques; +/-, <5 plaques irregular shape; -, zero plaques.

<sup>a</sup> Also tested with 100-times more phage, to amplify the signal; S427P showed (-), K414I and F426S showed (+/-), N451 K showed (+), wt showed cell debris (more plaques than could be counted).

1987; Wang *et al.*, 1993; Buchberger *et al.*, 1995), and because of the convenient location of the restriction sites. The unshaded part of Figure 1 represents the mutagenesis region.

After Mn PCR mutagenesis, individual mutant constructs were screened for their ability to support bacteriophage  $\lambda$  replication in a strain that is *dnaK* deficient, BB1553 (Bukau & Walker, 1990). BB1553 cells are deficient for  $\lambda$  replication; however, in the presence of a plasmid producing wtDnaK, the cells support  $\lambda$  propagation (Buchberger *et al.*, 1994a,b). After one round of Mn PCR mutagenesis, 100 DnaK constructs were screened for  $\lambda$  propagation activity, and all displayed wild-type  $\lambda$  propagation activity. Following two rounds of Mn PCR mutagenesis, 16 out of 100 clones were negative for  $\lambda$  replication and also expressed full-length DnaK. The DNA for each of the mutants was sequenced between bp 1214-1402. The majority of the plasmids sequenced contained mutations at multiple positions. Several of these mutant DnaK proteins were purified and characterized. On the basis of the observations obtained from the multiple-mutant proteins, several single mutants were constructed for further study. Table 1 shows the  $\lambda$  propagation activity of three multiple-mutant parents and several related single-site mutations. Four single-site mutants were found to be negative for  $\lambda$  propagation activity; K414I, F426S, S427P, and N451K, and were selected for further study.

### Increased concentrations of DnaK can rescue $\lambda$ activity of some mutant strains

Clones which were negative for  $\lambda$  replication were additionally tested to see if the mutant phenotype could be rescued by an increase in the intracellular concentration of DnaK. We reasoned that an increased amount of DnaK might rescue certain classes of biochemical phenotypes, pro-

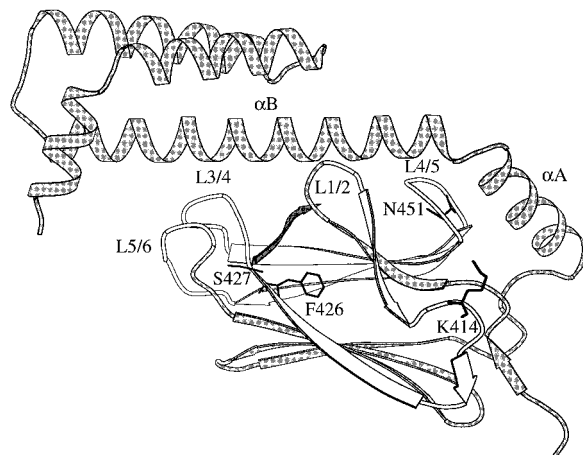


**Figure 1.** Ribbon diagram of the three-dimensional structure of C-terminal domain of DnaK (residues 389-607) derived from X-ray crystallography (Zhu *et al.*, 1996). Figure was drawn using MOLSCRIPT (Kraulis, 1991).

vided they are not too severe, such as: weak substrate binding, or weak co-chaperone interactions. An increased level of DnaK would not be expected to rescue mutations which dramatically interfere with the folded stability of the protein, or a specific domain interface (for example, between the nucleotide binding domain and the peptide binding domain).

The *dnaK* gene is in an expression plasmid (pMS) which contains a *tac* promoter, and hence is IPTG inducible. Western blots of whole-cell extracts probed with polyclonal antibodies against DnaK show that the expression level of pMS-DnaK in BB1553 cells without added IPTG is similar to that of a commonly used *E. coli* strain DH5 $\alpha$  containing the empty vector, pMS-EH (data not shown). The amount of DnaK synthesized increases by five- to tenfold during growth for one hour in 50  $\mu$ M IPTG (data not shown). Table 1 lists the results obtained when cells carrying various DnaK mutants were exposed to IPTG for 90 minutes prior to infection with bacteriophage  $\lambda$ . The S427P mutant cannot be rescued in this assay. Both F426S and N451K show moderate activity (+), while K414I shows minimal activity (+/-) in the presence of higher than normal DnaK concentrations. In summary, the *in vivo*  $\lambda$  assay results provide a rough ordering of the mutations from least severe to most severe: N451K = F426S < K414I < S427P.

### Position of the mutated residues

Two out of four of the single-site mutants which block  $\lambda$  propagation (F426S and S427P) are in the peptide binding site described in the co-crystal structure of the peptide binding domain of DnaK with peptide NRLLLTG (Figure 1; Zhu *et al.*, 1996). Position F426 contributes to the hydrophobic

**Table 2.** Structural summary of positions altered by mutagenesis based on X-ray crystal structure of a C-terminal fragment of DnaK (1DKX)

Residue	Location	Solvent accessibility	Hydrogen bonds <sup>a</sup> (Å)
K414	L 2/2a	0.1-0.4	K414:NZ to E444:OE1=2.74 (L 4/5)
F426	β-Strand 3	<0.1	426:N to I472:O=2.81 (β 6) 426:O to I472:N=2.92 (β 6)
S427	β-Strand 3	<0.1	S427:N to peptide R2:O=2.97 S427:O to peptide L4:N=2.88 S427:OG to T428N=2.72 (L 3/4) S427:OG to P470:O = 2.79 (L 5/6)
N451	L 4/5	<0.1	N451:ND2 to M408:SD=3.56 (β 2) N451:OD1 to R445:N=2.96 (L 4/5) N451:ND2 to R447:O=2.89 (L 4/5)

<sup>a</sup> Determined using Insight II.

pocket in which the central leucine (L<sub>4</sub>) binds. This large hydrophobic pocket is considered to be a crucial determinant of peptide binding (Zhu *et al.*, 1996). Replacement of the aromatic phenylalanine residue by the smaller serine residue would be expected to alter the hydrophobicity and volume of the L<sub>4</sub> binding pocket.

At the S427 position, the side-chain points away from the peptide binding site, yet S427 forms backbone-backbone hydrogen bonds with the bound peptide at residues R<sub>2</sub> and L<sub>4</sub> (for a list of hydrogen bonds see Table 2). In the structure, S427 has dihedral angles of  $\phi = -143$  and  $\psi = -173$ . Proline residues are known to impose a restriction on the backbone conformation such that  $\phi = -60(\pm 20)^\circ$ ; therefore, replacement of serine by proline would be expected to alter the backbone conformation of β-strand 3 as it goes through the peptide binding site, perhaps changing a multitude of interactions with the substrate. The fact that single mutations in either F426 or S427 abolish λ propagation activity indicates that the crystallographically defined peptide binding site is also critical to the *in vivo* functionality of the DnaK protein.

The single-site mutant K414I is close in tertiary structure to the area that sequentially attaches to the ATPase domain. It is near the interface between the β-sandwich domain and α-helix A. Position K414 is moderately solvent exposed (10-40%) in the crystal structure, and forms an electrostatic interaction with position E444 in loop 4/5 in the DKX peptide binding domain structure. The remaining mutation, N451K, is less exposed to solvent (<10%) and is in loop 4/5 of the β-sandwich domain. It forms hydrogen bonds between its side-chain atoms and the backbone atoms of two residues in loop 4/5 (R445 and R447).

### Global folded stability of mutant DnaK proteins

The loss of λ replication activity exhibited by each of the four mutants could be caused either by an alteration in the local chemistry of the site or by a global loss of folded structure. In order to distinguish between these two possibilities two techniques were used to monitor global changes in the

mutant proteins. Figure 2 shows circular dichroism spectra measured in the far-UV region as a monitor of overall secondary structure. The far-UV CD spectra of the mutant proteins are virtually overlapping and cross the ellipticity axis at the same wavelength as wtDnaK. This indicates that the mutant proteins have secondary structure which is very similar to that of wtDnaK.

The hydrodynamic properties of each of the mutant proteins were tested by size-exclusion chromatography at concentrations ( $\leq 0.1$  mg/ml) in which the monomer form of wtDnaK predominates (Schönfeld *et al.*, 1995). All of the mutant proteins had elution volumes which were identical with that of wtDnaK, indicating that none of the proteins is globally unfolded or predominantly oligomeric under these conditions (data not shown).

### Stability of individual folding/unfolding domains

Large molecular mass proteins the size of DnaK are often composed of several smaller folding domains (Privalov, 1982). In order to determine the stability of the smaller folding domains in the

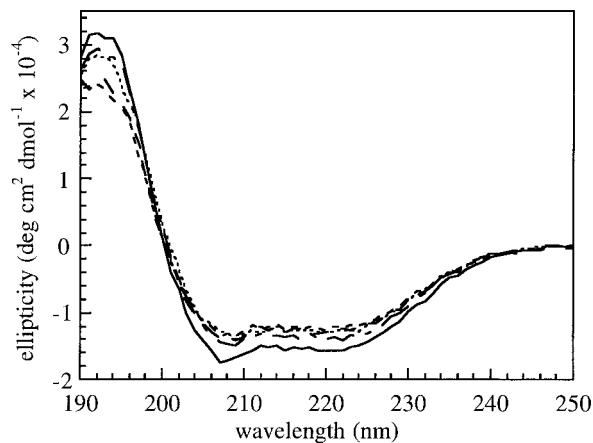


**Figure 2.** Circular dichroism of wtDnaK and mutants. wt, long broken line; K414I, short broken line; F426S, dot/dash line; S427P, dotted line; N451K, continuous line.

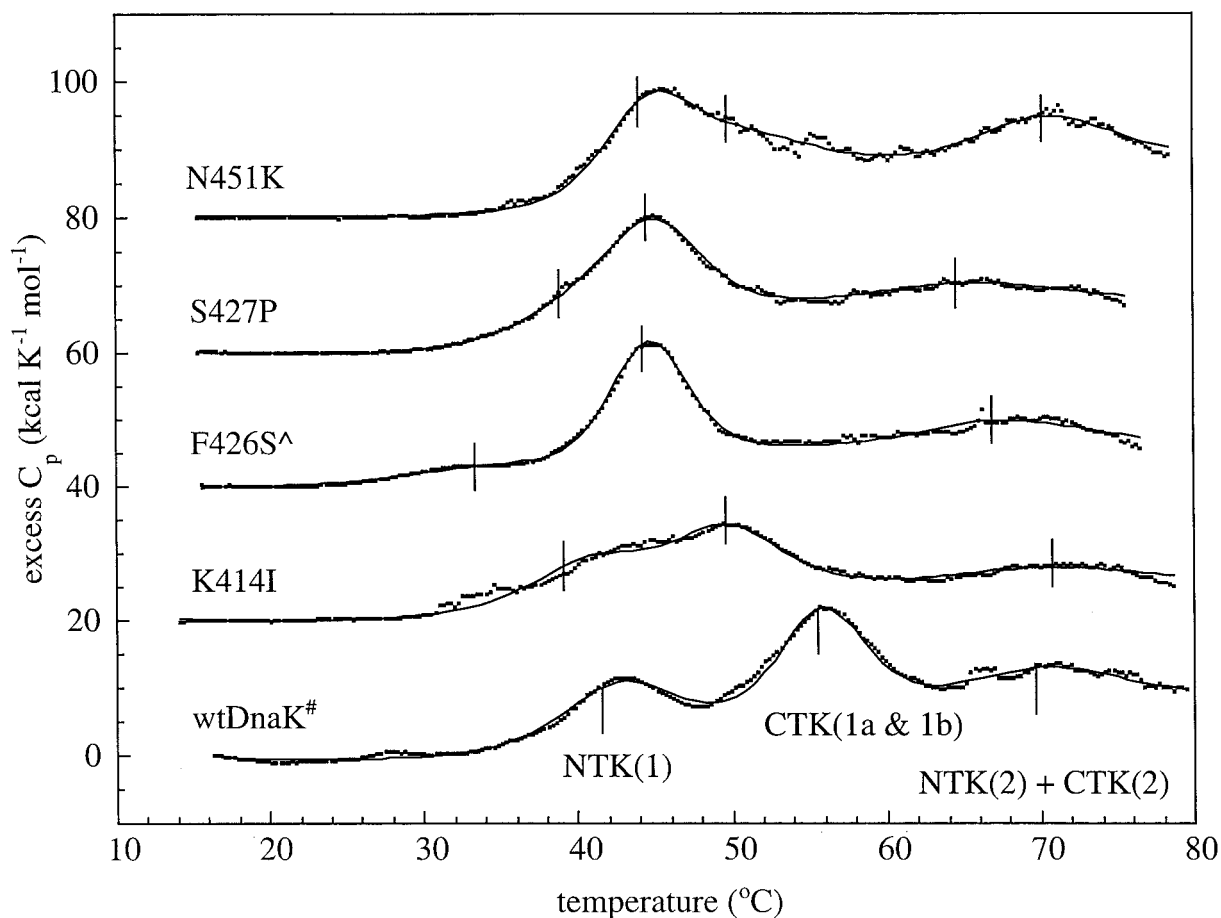


**Figure 3.** Differential scanning calorimetry of wtDnaK and mutants. The dots represent the data. The continuous lines reflect the best fit of the three-transition model to the data. Table 3 lists the best fit  $\Delta H$  and  $T_m$  values for each transition. Each mutant scan is incrementally offset by 20 kcal mol<sup>-1</sup> K<sup>-1</sup> for visibility. The notations # and ^ correlate data sets in the Figure with data sets in Table 3. The three short vertical lines on each scan graphically mark the best fit  $T_m$  values for each of the three transitions; these do not necessarily coincide with the  $C_p$  maxima due to the shift in the heat capacity baseline or  $\Delta C_p$ . The labels on the wtDnaK scan refer to the assignment of transitions in N and C-terminal fragments of the protein as discussed in the text.

DnaK mutants, the technique of differential scanning calorimetry (DSC) was used. DSC measures the amount of heat absorbed when a protein unfolds and allows determination of the  $T_m$ ,  $\Delta H$ , and  $\Delta S$  of each unfolding transition. For the DSC experiments a pH 9.0 buffer is used because the reversibility of the unfolding transitions and the solubility of the unfolded state are enhanced under these conditions. The folded stability of DnaK is not strongly pH-dependent between pH 7-10. For comparison, a DSC scan performed at pH 7.6 shows that the  $T_m$  values of DnaK are only 2-3 deg. C above those obtained at pH 9.0 (Montgomery *et al.*, 1993).

A DSC scan of wtDnaK at pH 9.0 is shown in Figure 3. At pH 9.0 the unfolding of the wt protein is 88% reversible, as determined by the  $\Delta H$  (area under the curve) obtained from an immediate rescan after scanning to 100°C. The wtDnaK protein has three visible peaks centered at 42°C, 55°C, and 72°C. Previous work has shown that the wtDnaK data can be well described by a four-state

(three-transition) model in which the heat capacity difference ( $\Delta C_p$ ) between each state is explicitly considered (Montgomery *et al.*, 1993). Based on DSC scans of two proteolytic fragments of DnaK, the three transitions of the intact protein have been assigned to N or C-terminal regions. The nomenclature for the assignments arises from the observation that the isolated N-terminal fragment has two transitions NTK(1) and NTK(2), while the C-terminal fragment displays three transitions CTK(1a), (1b), and (2). The first transition ( $T_m = 42^\circ\text{C}$ ) in full-length DnaK has been assigned to the majority of the N-terminal domain, NTK(1). The second transition ( $T_m = 55^\circ\text{C}$ ) has been assigned to the majority of the C-terminal portion of DnaK, CTK(1a & 1b). The third transition ( $T_m = 72^\circ\text{C}$ ) has components from both the N-terminal NTK(2) and C-terminal CTK(2) regions.

Figure 3 shows the DSC scans of the mutant DnaK proteins. In general, it is apparent that the middle transition, which corresponds to the majority of the C-terminal domain, is not located

**Table 3.** Fit thermodynamic parameters associated with DnaK folding domains

	NTK(1)		CTK (1a) and (1b)		NTK(2)+CTK(2)		$\chi^2$
	$T_m$	$\Delta H$	$T_m$	$\Delta H$	$T_m$	$\Delta H$	
wt*	42.6	76	55.8	91	72.2	65	
wt <sup>#</sup>	41.2	76	55.6	115	69.8	68	4.2e <sup>5</sup>
wt <sup>^</sup>	43.0	96	55.2	100	70.2	62	2.8e <sup>5</sup>
		obs (calc)		obs (calc)		obs (calc)	
K414I	39.1	66 (66-85)	49.5	88 (68-94)	70.7	52 (63-70)	5.2e <sup>5</sup>
F426S <sup>#</sup>	43.8	106 (79-98)	33.3	29 (10-35)	67.0	67 (56-64)	7.0e <sup>5</sup>
F426Sb	44.2	118 (80-99)	33.5	44 (11-36)	66.7	60 (56-63)	2.6e <sup>5</sup>
S427P	44.4	97 (81-100)	38.8	58 (30-55)	64.6	54 (52-60)	1.6e <sup>5</sup>
N451K	43.9	97 (80-98)	49.7	64 (69-95)	70.1	79 (62-69)	4.7e <sup>5</sup>

The  $T_m$  values are reported in deg. C;  $\Delta H$  values are in kcal mol<sup>-1</sup>. The symbols (# and ^) refer to multiple measurements of the specified protein and correlate with the symbols in Figure 3. The parameters marked with (\*) refer to data collected by Montgomery *et al.* (1993). An initial assignment of the observed transitions in the mutants to N or C terminal regions was based on the best agreement of the experimental  $\Delta H$  values of the mutants with the values calculated from the known transitions in wtDnaK, which have been corrected to the mutant  $T_m$  values using wtDnaK  $\Delta C_p$  values. This assignment process uses the known temperature dependence of  $\Delta H$ , and assumes that only the  $T_m$  value of each transition was significantly affected by the mutation. The numbers in parentheses represent a range of  $\Delta H$  values (minimum and maximum) calculated for each transition based on the three listed wtDnaK data sets. This range was calculated using the equation  $\Delta H_{(mut)} = \Delta H_R + \Delta C_p(R) [T_{m(mut)} - T_{m(R)}]$ . The R (reference state) refers to the wtDnaK data ( $T_m$ ,  $\Delta H$ , and  $\Delta C_p$ ).  $T_{m(mut)}$  refers to the best fit  $T_m$  value of the mutant;  $\Delta H_{(mut)}$  refers to the calculated  $\Delta H$  (minimum and maximum) expected for the mutant. The  $\Delta C_p$  values for each assigned transition were obtained from a previous study of wtDnaK:  $\Delta C_p$  NTK(1) = 2.8;  $\Delta C_p$  CTK(1a) and (1b) = 3.6;  $\Delta C_p$  (NTK2 & CTK2) = 1.7 kcal mol<sup>-1</sup> K<sup>-1</sup> (Montgomery *et al.*, 1993). In two cases, F426S and S427P, the best agreement between observed and calculated  $\Delta H$  values involved assigning the lowest temperature transition to the CTK(1a) and (1b) and the middle transition to the NTK(1). In the other two cases, K414I and N451K, the lowest temperature transition is assigned to NTK(1) and the middle transition is assigned to CTK(1a) and (1b).

at the same temperature in the mutant proteins, indicating that there is a change in the stability of the C-terminal domain. Figure 3 also shows the fits of a three-transition model to the data for each mutant, with short vertical lines representing the best-fit  $T_m$  values for each transition. In some cases (the middle transition in N451K for example), the best-fit  $T_m$  value does not coincide with the visually observed maximum in the data. This visual phenomenon occurs because the middle transition has been destabilized such that it has a  $T_m$  only ~6 deg. C higher than that of the lowest temperature transition. The maximum in the data at ~45.5 °C reflects the superposition of the areas of two transitions (43.9 and 49.7 °C) in a similar temperature range. The three-transition model is the simplest model which describes the data. Observed deviations from this model are not significant enough to invoke a four-transition model because they represent  $\Delta H$  values that are small enough to be within the error of the technique for this system ~15 kcal mol<sup>-1</sup> (see  $\Delta H$  values in Table 3 for repeated measurements of the same protein) and are in general, too small to reflect an unfolding domain. Table 3 lists the corresponding thermodynamic parameters obtained from these fits.

In general, the DSC data indicate that three of the mutant proteins (K414I, S427P, and N451K) are completely folded at 30 °C. In the F426S protein the CTK(1a) and (1b) domain has a  $T_m$  value of 33.5 °C; it therefore exhibits partial unfolding at 30 °C (<~25%) and at 24.5 °C (<~5%). It is important to note that the stability of wtDnaK is slightly higher at pH 7.6 than at pH 9.0; hence, the amount of partial unfolding is likely to be somewhat less at pH 7.6, where the biochemical assays were performed (Montgomery *et al.*, 1993). The observation

that the CTK(1a) and (1b) transition is significantly lower in all of the mutant proteins (<55 °C) correlates well with the general location of these four mutations.

### Peptide binding affinity of mutant DnaK proteins

hsp70 proteins are known to bind unfolded proteins (Liberek *et al.*, 1991b; Palleros *et al.*, 1991; Freeman *et al.*, 1995). Often small peptides are used as models of the unfolded state because most small peptides do not display folded structure and they make quantitative binding measurements simpler to perform (Flynn *et al.*, 1989; Schmid *et al.*, 1994; Jordan & McMacken, 1995). Each of the four mutant DnaK proteins was tested in a fluorescence anisotropy-based peptide binding assay to examine its substrate binding properties. The peptide APPY (CALLQSRLLLSAPRRRAATARY) was selected, based on the reported high affinity (63 nM) of a very similar peptide, APP (which has an A instead of a Y in the C-terminal position; Schmid *et al.*, 1994). Peptide APPY was fluorescently labeled on the N-terminal cysteine (F-APPY) with the sulfhydryl-reactive fluorescein conjugate 5-iodoacetamidofluorescein (5-IAF). The anisotropy assay follows the relative rotational diffusion of the fluorescein after excitation with polarized light. F-APPY should rotate in solution at a rate proportional to its molecular mass of ~3 kDa, and displays a modest anisotropy value. When F-APPY is bound and immobilized by DnaK, its molecular rotation is expected to be close to that of the larger molecule (70 kDa) and should display a significantly higher anisotropy value.

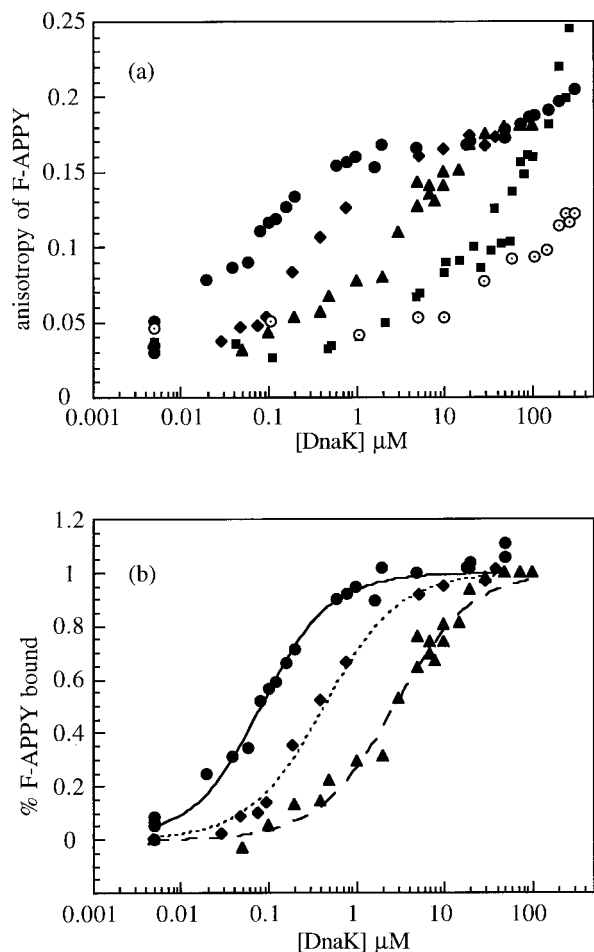


**Figure 4.** Peptide binding activity of wtDnaK and mutants. (a) Raw anisotropy values of the fluorescently labeled peptide F-APPY, as a function of increasing DnaK concentration. Filled circles represent wtDnaK, diamonds are K414I, triangles are F426S, squares are S427P, and dotted circles are N451K. (b) Best fit of a single-site binding model to the data. Filled circles represent wtDnaK, diamonds are K414I, triangles are F426S. Table 4 lists the  $K_d$  values associated with each fit.

The anisotropy change associated with the binding of F-APPY by increasing concentrations of wtDnaK is shown in Figure 4(a). The free F-APPY has an anisotropy value of  $0.048(\pm 0.012)$ ; the saturation region of the binding curve has an anisotropy value of  $0.171(\pm 0.004)$ . The anisotropy of the dye control, fluorescein- $\beta$ -mercaptoethanol, shows no change in the presence of DnaK (data not shown). This indicates that the dye itself has no affinity for DnaK in the range over which peptide binding is observed. The fluorescence intensity of F-APPY was also measured as a function of DnaK concentration and was found to be constant throughout the binding curve, suggesting that the local environment of the fluorescein does not change during the binding process. This is consistent with

**Table 4.** Peptide binding affinity of wtDnaK and mutants

	$K_d$ ( $\mu\text{M}$ )
wtDnaK	$0.06(\pm 0.02)$
K414I	$0.40(\pm 0.03)$
F426S	$2.70(\pm 0.2)$
S427P	$\approx 20^a$
N451K	$\approx 157^a$

<sup>a</sup> It was not possible to obtain a complete binding curve with these mutants.

Affinities were approximated by noting the concentration of the mutant at which the anisotropy value is similar to the value at the midpoint of the transition for wtDnaK.

the notion that the fluorescein does not bind in a hydrophobic pocket on DnaK.

Figure 4(a) also shows the behavior of the four single-site mutant proteins in this peptide binding assay. Two of the mutants, K414I and F426S, have high enough binding affinities so that the saturation region of the binding curve can be measured. The mutant S427P displays anisotropy values which are higher than wtDnaK in the plateau region, suggesting higher-order oligomerization than wtDnaK at these concentrations. Since the binding has not reached saturation in this range, the data could not be fit for a dissociation constant ( $K_d$ ). The mutant N451K binds even more weakly than S427P, shows an incomplete curve, and also could not be accurately fit. For the mutants S427P and N451K, the peptide binding affinity was approximated assuming that the plateau region anisotropy value would be the same as it is for wtDnaK.

Figure 4(b) shows the fits of a single-site binding model to the wtDnaK, K414I, and F426S data sets. Table 4 summarizes the  $K_d$  values obtained from these fits. The average of three wtDnaK binding experiments yielded a dissociation constant of  $0.075(\pm 0.025)$   $\mu\text{M}$ , which is in close agreement with the reported  $K_d$  of peptide APP (63 nM; Schmid *et al.*, 1994). The peptide binding affinity of K414I (0.4  $\mu\text{M}$ , Table 4) is only moderately reduced from wtDnaK, which is consistent with the fact that the mutation is not located in the crystallographically defined peptide binding site. Mutants F426S and S427P have considerably weaker affinities, with  $K_d$  values of 2.7  $\mu\text{M}$  and  $\approx 20$   $\mu\text{M}$ , respectively; these relative binding affinities correlate with the results from the  $\lambda$  propagation assay (Table 1). The mutant F426S can be partially rescued for  $\lambda$  activity at 50  $\mu\text{M}$  IPTG, whereas the mutant S427P cannot be rescued. The fact that these mutations, which are located in the structurally defined peptide binding site, dramatically affect peptide binding affinity confirms that this site plays a significant role in both the *in vitro* aspects of substrate binding affinity and in the functional aspects of *in vivo*  $\lambda$  DNA replication.

The fourth mutant, N451K, displays the weakest binding affinity of the group,  $K_d \approx 160$   $\mu\text{M}$ . This mutation is intriguing because it is not located in

**Table 5.** ATPase measurements of wtDnaK and mutants

	Steady-state	Steady-state + J/E
wt	0.108 ± 0.024)	7.682(±0.485)
K414I	0.370(±0.074)	5.125(±0.377)
F426S	0.249(±0.101)	3.226(±0.704)
S427P	0.094(±0.021)	2.835(±0.365)
N451K	0.620(±0.080)	5.036(±0.547)

Steady-state ATP hydrolysis units are mol ATP hydrolyzed mol<sup>-1</sup> DnaK per minute.

the known peptide binding site, but is in the innermost loop 4/5 near the junction of  $\alpha$ -helix A and  $\alpha$ -helix B. The DSC scan of the N451K protein indicates that it is completely folded at 24 °C and that its CTK(1a) and (1b) domain displays a  $T_m$  only 5 deg. C less than wtDnaK. In a previous study, mutations in DnaK were found that have weakened substrate affinity, and are also in or near loop 4/5, specifically G443D, G443S, and E444K (Burkholder *et al.*, 1996). One explanation is that the position of loop 4/5 is essential for the proper functioning of some aspect of the known peptide binding site. If  $\alpha$ -helix B forms a flexible hinge based on the rigidity of loop 4/5, then this region may influence how  $\alpha$ -helix-B covers the bound peptide. An additional possibility is that loop 4/5 is somehow involved in a second peptide binding site. Structural studies on loop 4/5 mutants of DnaK may address these possibilities.

### Intrinsic ATPase activity of DnaK mutants

Given that the ATPase activity of DnaK can be stimulated by polypeptide substrates, it seems clear that DnaK can be described as having allosteric properties (Gragerov *et al.*, 1994; Jordan & McMacken, 1995). The ATPase activity of each of the four single-site mutants was tested to assay if mutations in the peptide binding domain would also influence the activity of the ATPase domain, perhaps by altering an allosteric interface between the two parts of the protein. The wtDnaK protein displays a steady-state activity or turnover number of 0.108(±0.024) mol ATP hydrolyzed mol<sup>-1</sup> DnaK per minute at 30 °C using an enzymatic based colorimetric assay (Norby, 1988). This number compares well with the turnover number from the radioactive-TLC based assay (Liberek *et al.*, 1991a) for the same batch of wt protein: 0.096(±0.017) mol ATP hydrolyzed mol<sup>-1</sup> DnaK per minute. This turnover number is about two- to threefold higher than that obtained by other investigators: 0.030-0.045 mol ATP hydrolyzed mol<sup>-1</sup> DnaK per minute (Kamath-Loeb *et al.*, 1995; McCarty *et al.*, 1995).

The steady-state intrinsic ATPase activity for each of the four mutants is listed in the first column of Table 5. Three mutant proteins have steady-state ATPase values which are significantly higher than wtDnaK: K414I, F426S, and N451K. Although the structural mechanism of this process is not known, there are examples in the literature of mutations in DnaK which lead to elevated

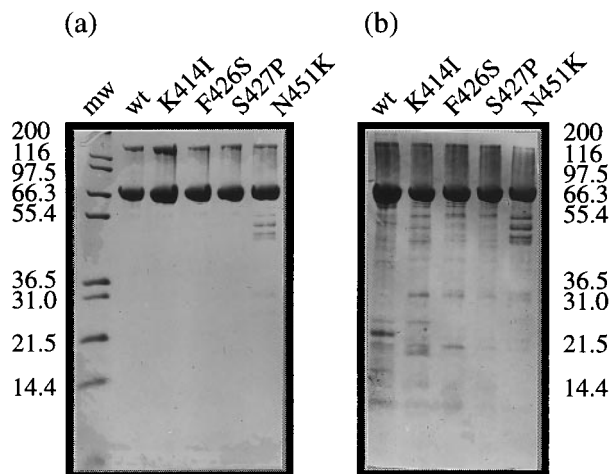


**Figure 5.** SDS-PAGE of purified wtDnaK and mutants. A 3.8  $\mu$ g sample of wtDnaK and mutants was loaded under (a) non-reducing conditions or (b) reducing conditions on 10% Tris-tricine-SDS/gels, electrophoresed and stained with either (a) Coomassie blue or (b) silver stain. Similar Coomassie stained gels run under reducing conditions show no bands above 70 kDa. Under non-reducing conditions, DnaK can form a small percentage of covalent dimer through the single cysteine in the protein, Cys15.

ATPase activity (Liberek *et al.*, 1991a; Buchberger *et al.*, 1994a; Kamath-Loeb *et al.*, 1995). One potential complication is the possibility that the high degree of ATPase activity displayed by the mutant proteins is due to trace amounts of a very active contaminating ATPase enzyme. In this regard, it should be noted that rather similar purification protocols were used for all proteins and that the addition of a final gel filtration step did not alter the ATPase activity of either wtDnaK or the K414I mutant. Figure 5 shows a SDS-PAGE gel of wtDnaK, with each of the four mutant proteins stained by Coomassie blue (a) and silver stain (b). N451K shows a small amount of 45-55 kDa species, but overall there is not an obvious contaminant band which tracks with the elevated ATPase activity.

To test the enzymatic purity of the mutant proteins, single turnover ATPase assays were performed. In this type of assay, the ATP concentration is kept at a minimum while the nucleotide-free protein concentration is present at saturating concentrations. Since only a limiting amount of ATP is present, enzymes with bound ATP can only turnover once. This type of experiment can measure how many different hydrolysis rate constants are observable (number of exponentials required to fit the data) and should also reflect the fraction of the total population giving rise to each rate constant (amplitude values associated with each exponential) assuming all species bind the ATP to an equivalent extent. For DnaK, the single-turnover ATP hydrolysis reaction has been shown to be well described by a first-order rate

equation (Karzai & McMacken, 1996; Theyssen *et al.*, 1996). If the single-turnover data cannot be fit to a single exponential process, the sample is not homogeneous with regard to enzymatic rates. The inhomogeneity could come from a contaminating ATPase or from enzymatically different populations of DnaK.

In this single-turnover ATPase assay, both wtDnaK and K414I displayed single exponential hydrolysis kinetics. The wtDnaK rate constant of  $0.038 \text{ min}^{-1}$  measured at  $24^\circ\text{C}$  is similar to that observed by other investigators (Karzai & McMacken, 1996). The fact that the K414I protein displays single exponential hydrolysis kinetics indicates that K414I is enzymatically pure. The observed rate constant for K414I ( $0.346 \text{ min}^{-1}$ ) is  $\sim$ ninefold faster than that of wtDnaK. The mutant proteins S427P, F426S, and N451K all display single-turnover kinetics which are best described by a two exponential fit. Both S427P and F426S contain a small amplitude component with a high hydrolysis rate constant, but the majority of the sample displays a rate constant close to that of wtDnaK. In contrast, for the N451K mutant a large fraction of the amplitude (79%) displays a fast hydrolysis rate constant, suggesting that the mutation itself is causing the elevated ATPase activity.

As an additional characterization of the K414I mutant, the  $K_m$  and  $V_{max}$  for ATP were determined (data not shown). The measured  $K_m$  was  $0.156 \mu\text{M}$ , with a  $V_{max}$  of  $0.417 \text{ mol ATP hydrolyzed mol}^{-1} \text{ DnaK per minute}$  at  $30^\circ\text{C}$ . This  $K_m$  value observed for K414I is somewhat lower than that of wtDnaK,  $1 \mu\text{M}$  (Kamath-Loeb *et al.*, 1995). This experiment indicates that the K414I mutant can functionally interact with ATP in roughly the same concentration range as wtDnaK.

### DnaJ and GrpE stimulation of mutant DnaK ATPase activity

The co-chaperone proteins DnaJ and GrpE have been shown to be required *in vivo* for  $\lambda$  replication activity (Georgopoulos *et al.*, 1990). It has also been shown that both co-chaperones and ATP are required for *in vitro* protein folding assays (Schröder *et al.*, 1993; Szabo *et al.*, 1994). Because all four of the single-site mutations show defects in  $\lambda$  propagation activity, it is possible that the deficiency could be in the ability of the mutant DnaK proteins to interact with either one or both of the co-chaperone proteins. One assay for co-chaperone interaction is the ability of DnaJ and GrpE to stimulate the ATPase of DnaK. Table 5 shows the steady-state ATPase activity of wtDnaK and each of the four mutants in the presence of DnaJ and GrpE. All of the mutants show some degree of co-chaperone stimulation, but none are as large as the wtDnaK. It is interesting to note that the two mutants which display the smallest degree of co-chaperone stimulation, F426S (42% of wtDnaK) and S427P (37% of wtDnaK), have substitutions in

the crystallographically defined peptide binding site.

### Peptide stimulation of ATPase activity

One assay for proper allosteric functioning of hsp70 proteins is polypeptide stimulation of the steady-state ATPase activity (Braell *et al.*, 1984; Flynn *et al.*, 1989; Sadis & Hightower, 1992; Jordan & McMacken, 1995). The results from this assay are a combination of two different phenomena, peptide binding in the presence of ATP and peptide stimulation of ATPase activity. It has also been shown for DnaK, and hsp70 proteins in general, that ATP reduces polypeptide binding affinity (Flynn *et al.*, 1989; Liberek *et al.*, 1991b; Schmid *et al.*, 1994), therefore the allosteric behavior of the weakest binding affinity mutants in this assay may be difficult to assess. The peptide used in this assay is NRLWLTG (NRW4) because of its high degree of solubility. This peptide is very similar to the peptide used in the co-crystal structure (NRLLLTG), and has been shown to bind to wtDnaK (Gragerov *et al.*, 1994) and to a tryptophan-less mutant of DnaK with a  $K_d \sim 0.14 \mu\text{M}$  (D.L.M. & L.M.G., unpublished data).

Figure 6(a) shows the ATPase activity of wtDnaK as a function of peptide NRW4 concentration. The activity increases sharply between 0 and  $200 \mu\text{M}$  peptide and plateaus at a level of  $\approx 0.55 \text{ mol ATP hydrolyzed mol}^{-1} \text{ DnaK per minute}$ . The peptide stimulated ATPase activity of K414I is also shown in Figure 6(a). The intrinsic ATPase activity of this mutant is already higher than wtDnaK (see Table 5), and the addition of peptide does not significantly change the activity level. Since the peptide binding assay showed that K414I has relatively high substrate binding affinity (see Table 4), it is likely that the peptide binds but cannot stimulate this mutant. This suggests that the K414I protein has altered allosteric interactions. Since different peptides were used in the peptide binding assay and the ATPase stimulation assay, there is a possibility that K414I cannot bind the NRW4 peptide. We feel this is a small possibility because wtDnaK can bind NRW4 and the K414I substitution is quite distant from the crystallographically defined binding site.

For comparison, the NRW4-stimulated ATPase activity of mutant F426S is shown in Figure 6(b). The intrinsic ATPase activity of F426S is higher than wtDnaK, but as increasing amounts of peptide are added the ATPase activity increases to the same plateau value as wtDnaK. This suggests that the allosteric interface is not disrupted in F426S. Interestingly, the NRW4 ATPase stimulation titration curve of F426S is surprisingly similar to that of wtDnaK, even though the two proteins have considerably different affinities ( $\sim 40$ -fold) for the F-APPY peptide in the absence of ATP. One straightforward explanation is that the NRW4 peptide has a similar binding affinity for F426S and wtDnaK in the presence of ATP. Another possi-

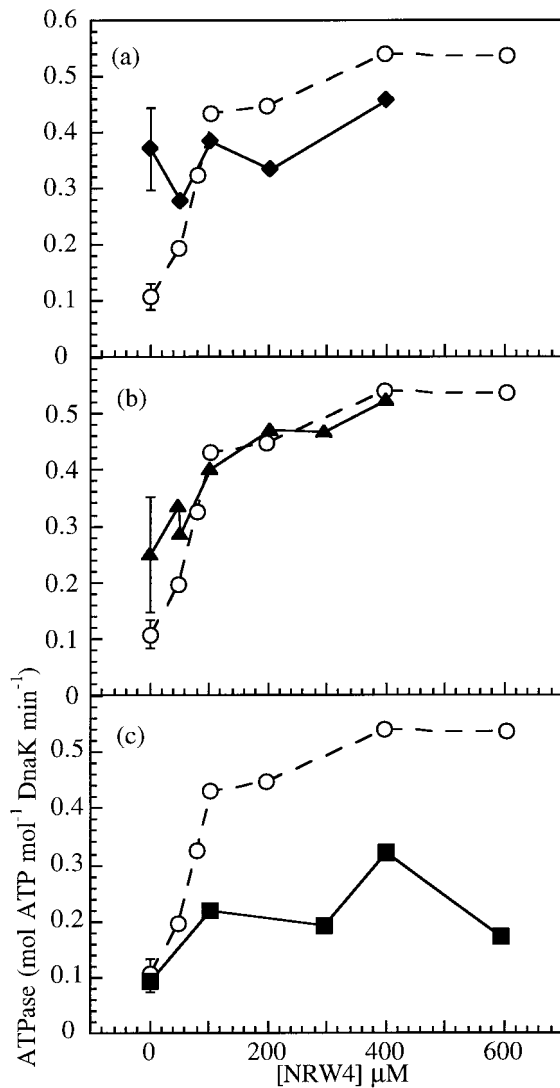


**Figure 6.** Peptide stimulated ATPase activity of wtDnaK and mutants. (a) wtDnaK (open circles) and K414I (filled diamonds). (b) wtDnaK (open circles) and F426S (filled triangles). (c) wtDnaK (open circles) and S427P (filled squares).

bility is that there is some sequence-specific interaction between NRW4 and the F426S mutant such that the degree of ATPase stimulation is higher than for wtDnaK, and compensates the stimulation curve such that it appears similar to the wt protein.

The behavior of a third mutant protein, S427P, is shown in Figure 6(c). S427P has an intrinsic ATPase activity similar to wtDnaK and upon addition of peptide the activity increases slightly but does not reach the plateau value of  $\approx 0.55$  mol ATP hydrolyzed mol<sup>-1</sup> DnaK per minute in the concentration range of peptide tested. This protein is known to have weakened substrate affinity (see Table 4), and it is possible that minimal stimulation is observed because only a small fraction of the peptide is bound. Given the inconclusive nature of

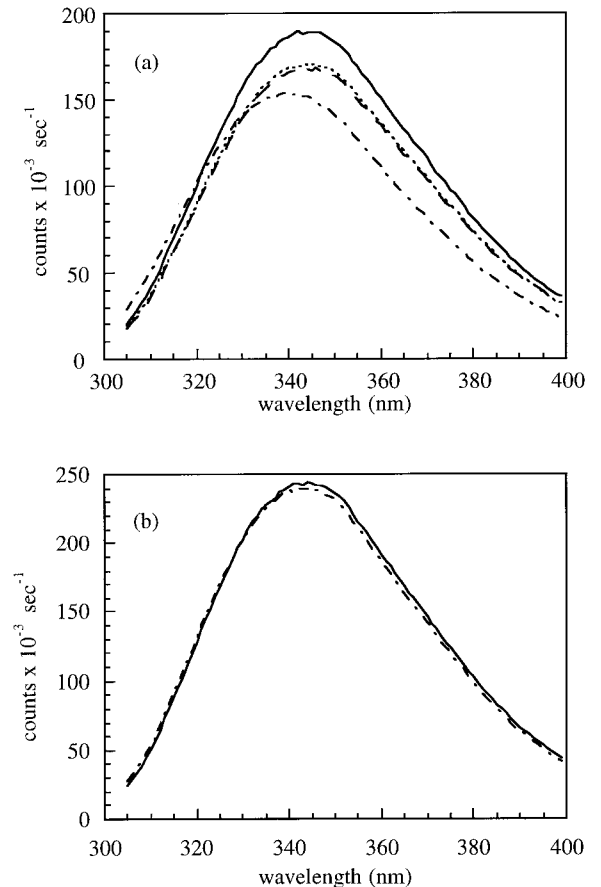


**Figure 7.** ATP-induced blue shift of Trp102 fluorescence for wtDnaK and K414I. (a) The continuous line represents wtDnaK with no added nucleotide, the dot/dash line represents wtDnaK with 0.48 mM ATP, the long broken line represents K414I mutant with no added nucleotide, and the dotted line represents K414I mutant with 0.48 mM ATP. (b) The continuous line represents N451K mutant with no ATP added and the dot/dash line represents N451K with 0.48 mM ATP.

the data with S427P, the mutant N451K with even weaker peptide affinity was not tested.

### Allosteric conformational change: ATP-induced blue shift of Trp102 fluorescence

To further examine the possibility that K414I has a defect in interdomain communication, a second type of allosteric assay was used. The addition of ATP to nucleotide-free DnaK induces a blue shift and a quench of the single tryptophan in the protein, W102, which is located in the N-terminal 45 kDa ATP binding domain (Palleros *et al.*, 1992; Banecki *et al.*, 1992). This spectral change has been shown to result from ATP binding, as opposed to ATP hydrolysis, because an ATPase-deficient mutant, DnaK-T119A, exhibits the same spectral change (Buchberger *et al.*, 1995; Theyssen *et al.*, 1996). This ligand-induced blue shift has additionally be shown to require the presence of about 150

amino acid residues from the C-terminal domain. Since a portion of the C-terminal domain influences the blue shift of W102, this spectral change can be thought of as a signature of interaction between the ATPase domain and the substrate binding domain and hence, can be considered an allosteric assay. Figure 7(a) shows the behavior of K414I and wtDnaK in this ATP-induced blue shift assay. It is useful to note that the ATP concentration is 120-fold higher than the DnaK concentration. Even though the steady-state ATPase activity of K414I is three times higher than wtDnaK, the hydrolysis is not fast enough to significantly deplete the ATP concentration during the time-course of the experiment (five minutes). While wtDnaK displays the characteristic blue shift and quench upon addition of ATP, the mutant K414I exhibits neither phenomenon. This observation provides a second line of evidence that K414I has a dysfunctional allosteric interface. Figure 7(b) shows that a second mutant protein, N451K, also does not display any change in its tryptophan fluorescence upon the addition of ATP. Mutants F426S and S427P behave like wtDnaK (data not shown). The fact that mutant N451K is defective in this ATP dependent spectral change suggests that N451 may also be involved in communication between domains.

### ATP-induced weakening of peptide binding affinity

A third assay was used to address proper allosteric function in the DnaK mutants. As a complement to the peptide-stimulated ATPase assay, it is known that the binding of ATP can weaken the affinity of DnaK for polypeptide substrates (Flynn *et al.*, 1989; Liberek *et al.*, 1991b; Schmid *et al.*, 1994). Given that ATP reduces the affinity for polypeptide substrates, it should be noted that the degree of peptide substrate release will be influenced by the amount of DnaK in the assay. This experiment was designed such that each mutant was tested at concentrations where ~30-90% of the peptide is bound in the absence of ATP. Concentrations in the saturation region of the binding isotherm were avoided because they show a smaller signal change upon adding ATP. Figure 8(a) shows a kinetic trace of the binding of F-APPY peptide to wtDnaK and K414I after the addition of ATP. The anisotropy value of peptide F-APPY is used to monitor peptide binding, as it was in the peptide binding affinity assay (Figure 4(a)). When ATP is added to the pre-bound mixture of wtDnaK and F-APPY the anisotropy value drops, reflecting a smaller fraction of peptide bound. Conversely, when ATP is added to a pre-bound K414I and F-APPY mixture, the anisotropy level does not change significantly. This is a third line of evidence that K414I is an allosteric mutant.

Figure 8(b) shows the anisotropy level attained by wtDnaK and each of the four mutants ten minutes after the addition of ATP. Upon ATP addition,

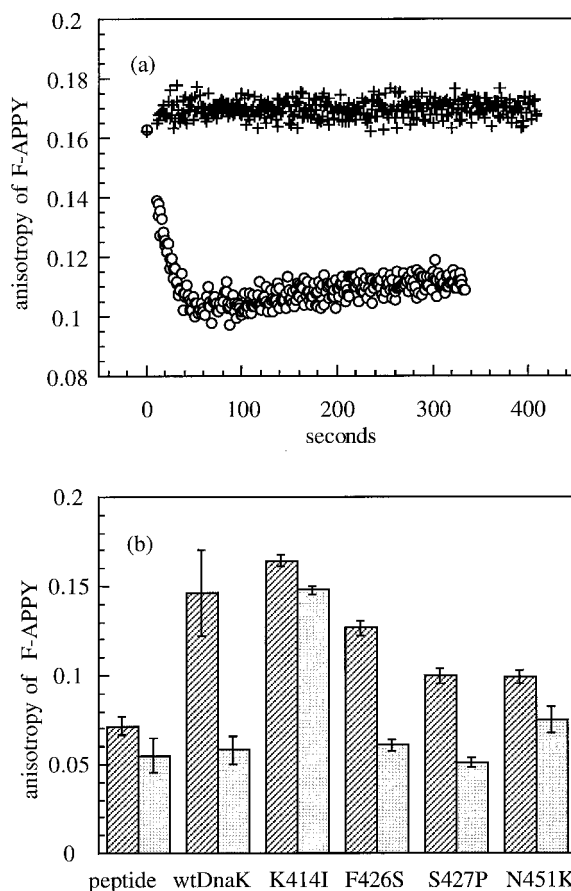


**Figure 8.** ATP-induced weakening of peptide binding affinity in wtDnaK and mutants. (a) Kinetics of ATP-induced peptide release (decrease of F-APPY anisotropy). Circles, wtDnaK (5  $\mu$ M); +, K414I (5  $\mu$ M). The ATP (0.55 mM) was added at time zero. (b) Equilibrium measurement of ATP-induced peptide release (decrease of F-APPY anisotropy). The diagonal striped bars show the anisotropy of peptide F-APPY without ATP in the absence and presence of wtDnaK or a mutant as indicated. The shaded bars show the anisotropy value that results ten minutes after the addition of 0.48 mM ATP. The error bars indicate the standard deviation from the mean of three measurements. Protein concentrations were: wtDnaK (1.0  $\mu$ M), K414I (0.98  $\mu$ M), F426S (5.5  $\mu$ M), S427P (30.2  $\mu$ M), and N451K (60.0  $\mu$ M) to account for differences in peptide binding affinity.

the two peptide binding site mutants F426S and S427P show peptide anisotropy levels that are similar to that of free peptide, suggesting that they have normal allosteric function. At the protein concentrations used in this experiment the N451 K-F-APPY complex shows a similar anisotropy value as the S427P-F-APPY complex, but when ATP is added the N451K does not show the same degree of ATP-induced peptide dissociation. This inefficient release of peptide in ATP is a second line of evidence that N451K may have altered allosteric behavior.

## Discussion

This study used a random mutagenesis approach combined with a screen for *in vivo* function to identify mutations in the peptide binding domain of DnaK. The single-site mutants which are negative for bacteriophage  $\lambda$  propagation activity can be grouped into two categories based on their location: (1) mutations outside of the peptide binding site (K414I and N451K); and (2) mutations in the structurally identified peptide binding site (F426S and S427P). The first class of mutations are near the edge of the  $\beta$ -sandwich domain near  $\alpha$ -helix A and have an affect on allosteric interactions. The data from the K414I mutant, in particular, strongly identifies this position in the peptide binding domain as a key region involved in interdomain coupling. The second class of mutations involves residues that contribute to the peptide binding site and display a lower substrate binding affinity. In the process of characterizing these two categories of mutants, two additional trends emerged. In a mutant that is defective in allosteric interactions, K414I, the ATPase activity is significantly higher than wtDnaK. These data suggest that this allosteric mutation influences the enzymatic activity of the N-terminal ATPase domain. Lastly, it was observed that proteins with mutations in the peptide binding site showed the weakest ATPase stimulation by DnaJ and GrpE, <42% of wtDnaK, suggesting that at least one of the co-chaperone proteins interacts with DnaK through the structurally identified peptide binding site.

### Allosteric mutations

There are several lines of evidence which lead to the conclusion that the K414I mutant has an altered allosteric interface between the two functional domains of the protein. The first line of evidence is that although this protein has only slightly altered peptide binding affinity (~ sixfold weaker than wt), it does not display peptide stimulation of ATPase activity (Figure 6(a)). Secondly, K414I cannot perform the well-characterized ATP-induced conformational change (Palleros *et al.*, 1992; Banecki *et al.*, 1992; Buchberger *et al.*, 1995). Upon addition of ATP, the wtDnaK shown in Figure 7(a) exhibits a blue shift and quench of W102 (located in the N-terminal domain), while the K414I mutant exhibits no change. Interestingly, the K414 position in the wt protein was also identified in a protease digestion and N-terminal sequencing study as a trypsin-accessible site which shows an increase in accessibility in the presence of ATP (Buchberger *et al.*, 1995). Thirdly, addition of ATP to K414I does not induce peptide release (Figure 8(a) and (b)). ATP can still functionally interact with the K414I because the measured  $K_m$  value for ATP is 0.1  $\mu$ M, while that of wtDnaK is 1  $\mu$ M (Kamath-Loeb *et al.*, 1995). Finally, the ATPase activity of K414I is considerably higher

than that of wtDnaK (Table 5). The fact that a mutation in the C-terminal domain can influence the enzymatic activity of the N-terminal domain implies that the interdomain interface does not function in the same manner as in the wt protein.

The second mutant in this class, N451K, is considerably more complex. Although it is not located in the peptide binding site, it nevertheless displays the weakest binding affinity (Table 4). The three techniques used to address global structural stability (CD, gel filtration, and DSC) all indicate that the N451K protein is folded. The strongest line of evidence that N451K has an allosteric defect is that it exhibits no change in W102 fluorescence when ATP is added (Figure 7(b)). This mutant additionally shows a significantly higher steady-state ATPase activity (Table 5). Single-turnover analysis indicates that the enzymatic activity comes from two species with the larger component (79%) having the high single-turnover activity. Based on the SDS-PAGE of this sample, the majority of the protein present is the 70 kDa band (Figure 5). This band is also recognized by an anti-DnaK polyclonal antibody on a Western blot (data not shown), arguing that the higher activity comes from the N451K mutant protein. This would be consistent with the observation that some allosteric mutants, like K414I, have elevated ATPase activities. Moreover, N451K exhibits less peptide release when ATP is added than the S427P mutant (Figure 8(b)). The weak peptide binding affinity of this mutant (Table 4) admittedly makes the allosteric functionality difficult to assay rigorously, yet it is also rather intriguing that a mutation so far away from the known peptide binding site actually has such a dramatic effect on substrate binding *in vitro*. Surprisingly, when assayed for  $\lambda$  propagation *in vivo*, this mutant can be rescued by overexpression of the protein (Table 1), suggesting that the mutant can be adjusted, perhaps by co-chaperone proteins, into a semi-functional conformation *in vivo*.

The two C-terminal domain allosteric mutants presented here show some similar traits to previously studied allosteric mutants such as E171(A, L, K), and D201N (Wild *et al.*, 1992; Buchberger *et al.*, 1994a; Kamath-Loeb *et al.*, 1995). These two positions are both in the N-terminal domain near the ATP binding site, located inside the cleft between sub-domains I and II. Mutants at the E171 position could not perform the *in vivo*  $\lambda$  propagation assay and exhibited the *in vitro* phenotypes of: (1) elevated steady-state ATPase rates; (2) relatively normal peptide binding activity, but no peptide stimulation of ATP hydrolysis; (3) no ATP-induced peptide release; and (4) no ATP-induced conformational change. The N-terminal domain mutant D201N showed no *in vivo*  $\lambda$  propagation, normal peptide binding but no peptide stimulation of ATPase activity, no ATP-induced conformational change, and also minimal ATP-mediated release of GrpE from DnaK (Kamath-Loeb *et al.*, 1995).

Previous studies, such as those on the DnaK756 mutant, have identified residues in the C-terminal

domain which may be involved in allosteric function. The DnaK756 protein is a triple mutant (G32D, G455D, and G468D; Miyazaki *et al.*, 1992) which displays several of the biochemical phenotypes observed in E171 K (Liberek *et al.*, 1991a,b). Notably, the positions G455 and G468 are not in the same structural area as K414I and N451K. G455 is on the back of the  $\beta$ -sandwich in  $\beta$ -strand 5. G468 is at the top of loop 5/6 near R467, which is an ATP-induced conformationally accessible trypsin cleavage site that may play a role in the positioning of the  $\alpha$ -helix B over the peptide binding site (Buchberger *et al.*, 1995; Rüdiger *et al.*, 1997a). The only apparent connection between these positions and the mutants located at the edge of the  $\beta$ -sandwich is that positions K414, N451, and G468 are close to  $\alpha$ -helical regions A and B, suggesting that the helical domain may play a role in allosteric function by regulating access to the peptide binding site (the "latch hypothesis"; Zhu *et al.*, 1996). Additionally, it has been shown that a mutation, E543K, can alter interdomain communication in bovine hsp70 (Ha *et al.*, 1997). In summary, although there are now several mutations which disrupt allosteric functionality, there is not as yet enough data to propose a model or map an interaction surface between the two ligand binding domains of DnaK. Indeed, there may be several key positions throughout the molecule which are necessary for correct allosteric functionality, yet are not directly part of the contact interface between the ATPase domain and the polypeptide substrate binding domain.

### Mutations in the peptide binding site

The mutant proteins with substitutions in the known peptide binding site appear to have their primary biochemical defect in peptide binding. The crystal structure of a C-terminal fragment of DnaK (residues 389-607) with bound peptide (NRLLLTG) describes the structural elements involved in peptide binding (Zhu *et al.*, 1996; for a review, see Rüdiger *et al.*, 1997a). The peptide is bound in an extended conformation as deduced from transferred nuclear Overhauser experiments (Landry *et al.*, 1992); the leucine in position 4 of the peptide is completely buried in a deep pocket pointing toward the center of the  $\beta$ -sandwich formed by F426, V436, I438, I401, and T403. In the F426S mutant it is likely that this pocket loses a considerable amount of its hydrophobic character, which may explain its weaker substrate binding affinity ( $\sim 36$ -fold lower than wtDnaK). The bound peptide forms seven main-chain hydrogen bonds with DnaK residues in the binding site. S427 in wtDnaK forms two of the seven peptide-DnaK hydrogen bonds using its backbone atoms. Replacement of S427 ( $\phi = -143^\circ$ ) by proline ( $\phi = -60(\pm 20)^\circ$ ) would not only make one peptide-DnaK hydrogen bond impossible to form, but also would alter the backbone conformation of loop 3/4 as it passes through the binding site which may disrupt

additional interactions. The net effect of S427P substitution is a dramatic weakening of substrate binding affinity ( $\approx 270$ -fold).

The *in vivo*  $\lambda$  propagation data are consistent with the relative ordering of the severity of these two mutants. F426S binds peptide more tightly than S427P *in vitro* and can be partially rescued *in vivo* by increasing the intracellular concentration of F426S protein, whereas S427P cannot be rescued. Mutation of positions F426 and S427, both previously structurally identified as being critical for peptide binding, are shown in this study to interfere with both peptide binding in solution and  $\lambda$  replication activity *in vivo*. Taken together, the data from these two mutants provide functional evidence to support the structural identification of the polypeptide substrate binding site in DnaK.

### Co-chaperone interactions

All of the mutant DnaK proteins were tested for ATPase stimulation by the co-chaperone proteins DnaJ and GrpE. The data show (Table 5) that the proteins with the weakest co-chaperone ATPase stimulation values ( $< \sim 42\%$  of wtDnaK) are also mutated in the peptide binding site. This may imply interaction of co-chaperone(s) with DnaK through the known peptide binding site or, alternatively, that the binding site mutants cannot perform a particular conformational change in response to co-chaperones.

This study does not identify which co-chaperone interacts with the peptide binding site of DnaK, but data supporting an interaction with DnaJ exists in the literature. In general, DnaJ is known to enhance the ATP hydrolysis rate of DnaK and to stabilize peptide substrate binding to DnaK in the presence of ATP (Liberek *et al.*, 1991a; Langer *et al.*, 1992; McCarty *et al.*, 1995; Wawrzynów *et al.*, 1995). Studies have shown that saturating concentrations of fragments of DnaJ (residues 1-75) in conjunction with peptides known to bind well to DnaK (peptide C) can stimulate the ATPase of DnaK to similar levels as are attained with wtDnaJ (Karzai & McMacken, 1996). This study suggests that DnaJ interacts with the polypeptide binding site of DnaK in the stimulation process. Additional evidence exists that DnaJ may require a specific conformational state of the N-terminal domain of DnaK for productive interaction. Two N-terminal domain mutations E171 K and D201N show no ATPase stimulation in the presence of DnaJ, although the proteins are capable of hydrolyzing ATP in the absence of DnaJ (Kamath-Loeb *et al.*, 1995). The site(s) on DnaK which interact with DnaJ are not completely established, but given that DnaJ can influence the activities of two different domains of DnaK, it seems plausible that DnaJ could interact with both domains.

The function of the GrpE protein is to mediate nucleotide release from DnaK (Liberek *et al.*, 1991a; Wu *et al.*, 1996; Packschies *et al.*, 1997). Much is known about the structural nature of the inter-

action between DnaK and GrpE from the co-crystal structure of GrpE (residues 34-197) and the N-terminal domain of DnaK (Harrison *et al.*, 1997). The two proteins contact each other in six places, including the loop near Gly32 in DnaK which was previously shown to be necessary for stable binding and co-chaperone stimulation activity (Buchberger *et al.*, 1994b). Intriguingly, the GrpE structure contains a very long  $\alpha$ -helix which extends beyond the N-terminal domain, potentially near the C-terminal domain; however, it is currently unknown if GrpE has any functional interaction with the C-terminal domain of DnaK. Further studies with the two peptide binding site mutants, F426S and S427P, may help elucidate whether or not co-chaperone proteins interact with the peptide binding site of DnaK.

## Materials and Methods

### Reagents

Primers were obtained from Northwestern Biotechnology Facility, Gibco BRL, and Integrated DNA Technologies, Inc. Restriction enzymes were from New England Biolabs. Dialysis membranes were from Spectrum Medical Industries Inc. BioRad Silver Stain Plus and agarose were purchased from BioRad. Buffers, antibiotics, IPTG, ATP,  $\beta$ -NADH, phosphoenolpyruvate (PEP), and pyruvate kinase (PK)/lactate dehydrogenase (LDH) enzymes were all purchased from Sigma.

### Random mutagenesis

Random mutagenesis of the DnaK region bp 1214-1402 (amino acid residues 405-468) was performed by Mn PCR (Cadwell & Joyce, 1994). The PCR reaction was performed using *Taq* polymerase (Perkin Elmer), pMS-DnaK as a template, and primers corresponding to bp 1147-1150 (5' primer) and bp 1898-1914 (3' primer) of the wtDnaK sequence. This ~700 bp fragment was made as a precursor to the final 188 bp insert to enable confirmation of restriction enzyme cleavage. The product of the first round of PCR was run on an agarose gel, gel purified, concentration estimated, and then diluted to  $2 \times 10^{-10}$  M for use as a template for a second round of PCR mutagenesis using the same primers. The PCR product from the second round of mutagenesis was then digested with *NcoI* and *SphI* to produce a 188 bp fragment which was gel purified and inserted into pMS-DnaK using the same restriction sites.

### Plasmid constructions

The pMS-DnaK construct was made by excising the DnaK coding region and 5' ribosome binding site from plasmid pJZ515 (generous gift of C. Georgopoulos) by digestion with *XbaI* and *HindIII* and subcloning it into the prokaryotic expression vector pMS-EH cut with the same enzymes. pMS-EH contains a *tac* promoter upstream of the multiple cloning site, and also *lacI<sup>q</sup>* to produce *lac* repressor allowing IPTG-inducible expression. This plasmid confers ampicillin resistance. A pGEM-DnaK construct (pGEM-3Zf(+), Promega) was made in a similar fashion for use in subcloning procedures.

The single-site mutant N451K arose naturally in the mutant screen. The single mutants F426S and S427P were made by subcloning a ~100 bp *NcoI*-*BstEII* fragment out of a multiple mutant and inserting it into pGEM-DnaK at the same sites. The entire *dnaK* gene was then subcloned into the pMS-EH expression vector using *XbaI* and *HindIII*. The single mutant K414I was made by site directed mutagenesis. A PCR fragment was generated using PFU (Stratagene), the pMS-DnaK template, and a mutagenic primer 5'*NcoI*K414I: 5' (TAT CGA AAC CAT GGG CGG TGT GAT GAC GAC GCT GAT CGC GAT AAA CAC CAC) 3' and a 3' primer corresponding to the 1475-1498 bp region of DnaK. This fragment was cut with *NcoI* and *SphI* and inserted into pGEM-DnaK at the same sites, and then the entire *dnaK* gene was subcloned into pMS-DnaK using *XbaI* and *HindIII*. The region between bp 1214-1402 (*NcoI* and *SphI* sites) was sequenced for all four mutants using the dideoxy chain termination method with the Oncor Fidelity sequencing kit (Applied).

### Bacteriophage $\lambda$ propagation assays

The  $\lambda$  propagation assays were performed in BB1553 cells (MC4100  $\Delta$ *dnaK52::Cm<sup>r</sup> sidB1*) which are *dnaK*<sup>-</sup> (a generous gift from B. Bukau; Bukau & Walker, 1990). The  $\lambda$  strain  $\lambda$ KH54, which prevents lysogenization (Sambrook *et al.*, 1989), was used for all assays. All  $\lambda$  propagation assays were performed on LB plates in the presence of 25  $\mu$ g/ml chloramphenicol and 100  $\mu$ g/ml ampicillin. Bacteriophage infections were performed on cultures of at least  $A_{600} = 1$  for 20 minutes at room temperature, followed by plating and growth at 30°C. For studies in the presence of IPTG, cells were grown to  $A_{600} = 1$  at 30°C, IPTG was added to 50  $\mu$ M and the growth was continued for 90 minutes. The cells were then infected with  $\lambda$  and plated with top agar containing 50  $\mu$ M IPTG. All other properties of the  $\lambda$  assay were performed according to standard protocols at 30°C (Sambrook *et al.*, 1989).

### Protein purification

Both wt and mutant forms of DnaK were overexpressed by IPTG induction of pMS-DnaK. The wtDnaK was grown in BL21 cells at 37°C. Mutant forms of DnaK were overexpressed in BB1553 cells and grown at 30°C. Soluble protein extracts were prepared at 4°C by lysozyme treatment and sonication, followed by centrifugation at 17,400 g for 30 minutes. All subsequent purification steps were performed at 4°C. The wtDnaK and the mutant N451K were purified by a three column procedure: DEAE Sepharose anion exchange, ATP-agarose, and Resource Q anion exchange. Mutants K414I, F426S, and S427P were purified by a two column procedure: Q-Sepharose anion exchange and ATP-agarose. Gel filtration (Tso Haas TSK-G4000 7.8 mm  $\times$  30 cm), when performed as discussed in the text, was performed in HMK buffer (20 mM Hepes, 100 mM KCl, 5 mM MgCl<sub>2</sub>, pH 7.6) at 24°C.

Soluble protein extracts were loaded on the first anion exchange column which was equilibrated in 20 mM Tris-HCl, 0.1 mM EDTA (pH 6.9 at 24°C), and eluted with a 50 mM-350 mM NaCl gradient over five column volumes. Peak fractions containing 70 kDa protein were pooled, MgCl<sub>2</sub> added to 5 mM final, and recirculated over a 20 ml ATP-agarose column (Sigma: C-8 linkage) pre-equilibrated in 20 mM Tris, 5 mM MgCl<sub>2</sub>, 100 mM

NaCl (pH 7.0). The column was washed with 2.0 M NaCl, 20 mM Tris (pH 7.0), to remove non-specific binding, re-equilibrated back to 100 mM NaCl, then eluted with two column volumes of 5 mM ATP in the same buffer. After the DnaK and ATP were rinsed from the column, the ATP affinity column procedure was routinely repeated two more times to remove the majority of DnaK in the extract. After use, the ATP-agarose column was washed with buffered 4 M GuHCl to prevent cross-contamination of proteins. The three ATP elutions of DnaK were pooled and the ATP was removed by repeated concentration/dilution with 20 mM Tris, 100 mM NaCl, 10 mM EDTA (pH 7.0) in a 250 ml Amicon ultra filtration cell, followed by dialysis against the same buffer until the 260/280 nm absorption ratio was below  $\approx 0.7$ . Accurate measurements of optical density were performed at low ( $\sim 0.1$  mM) concentrations of EDTA.

When the 30 ml Resource Q column was run, it was pre-equilibrated in 20 mM Tris, 0.1 mM EDTA (pH 7.0), and eluted with a seven column volume gradient of 50 mM–400 mM NaCl. If the sample contained any nucleotide-bound DnaK, that species eluted first, closely followed by nucleotide-free DnaK, which at high concentrations eluted as a doublet of peaks. The purity of all samples is shown in Figure 5. All DnaK-containing fractions were checked for 260/280 nm absorption, and only those with ratios  $< 0.70$  were considered to be nucleotide free and used for experiments. Pure DnaK was concentrated to at least  $\approx 10$  mg/ml and the buffer exchanged for HMK buffer in a Centricon-10 concentrator (Amicon) prior to quick freezing with liquid nitrogen and storage at  $-80^\circ\text{C}$ . An extinction coefficient of  $\epsilon_{280} = 15.8 \times 10^3 \text{ M}^{-1} \text{ cm}^{-1}$  was used for wtDnaK (Jordan & McMacken, 1995) and the four single-site mutants.

### Circular dichroism

Circular dichroism spectra were obtained using a 0.1 cm cuvette in a Jasco J-715 spectropolarimeter. The collection parameters were 1 nm band width, 1 nm step size, 10 nm  $\text{s}^{-1}$  and a four a second response time. Experiments were performed at  $24^\circ\text{C}$  in 10 mM sodium borate (pH 9.0) at 0.1–0.2 mg/ml protein and normalized for protein concentration.

### Differential scanning calorimetry

DSC scans were performed on a MCS-DSC (Microcal) on samples that had first been dialyzed overnight against 25 mM glycine (pH 9.0), and degassed for 20 minutes prior to loading the instrument. Buffer from outside the dialysis bag was loaded in the reference cell of the calorimeter. Samples (2.5 mg/ml) were scanned at  $60^\circ\text{C}$  per hour. Data were analyzed using the Origin 2.9-DSC module (Microcal Software) and fit using a three transition with  $\Delta C_p$  model, in which each transition is modeled as a two-state transition.

### Fluorescein labeling of peptide APPY

Peptide CALLQSRLLSAPRRAAATARY (APPY) was synthesized, purified, and subjected to mass spectroscopy for confirmation of molecular weight at the Genetic Engineering Facility, University of Illinois Biotechnology Center. For labeling, APPY was dissolved in 10 mM ammonium bicarbonate buffer (pH 7.5; buffer B) at 14 mg/ml, checking the concentration by tyrosine

absorbance using an extinction coefficient of  $1400 \text{ M}^{-1} \text{ cm}^{-1}$  (Creighton, 1993). APPY was initially treated with a tenfold molar excess of DTT at  $25^\circ\text{C}$  for 30 minutes to reduce intermolecular disulfides. The DTT was removed by gel filtration in buffer B on 1 cm  $\times$  25 cm column of G-25 Sepharose (Pharmacia). Fluorescent labeling was performed on the reduced peptide at 40  $\mu\text{M}$  APPY with a fivefold molar excess of 5-IAF (Molecular Probes) in buffer B at  $25^\circ\text{C}$  for two to three hours with stirring, in darkness. Excess free 5-IAF was removed by gel filtration on a 1 cm  $\times$  50 cm G-25 Sepharose column in buffer B. Fractions containing F-APPY were pooled, lyophilized, re-dissolved in water, and purified from minor contaminants by reverse-phase chromatography on a C18 column (Vydac 218TP54), monitored at 212, 274 and 492 nm. It was independently determined that fluorescein-mercaptoethanol and reduced APPY eluted much earlier and would be well resolved from F-APPY; however, oxidized APPY eluted much closer. In order to separate any remaining unlabeled oxidized APPY in the F-APPY stock, samples were reduced with 1 mM DTT prior to loading the C18 column. The primary fluorescein-labeled peptide peak was pooled, lyophilized, and resuspended in 20 mM Tris (pH 8.5) with a maximum solubility of  $\sim 12 \mu\text{M}$ . The overall yield was on the order of 0.7%. The concentration of the peptide was assumed to be the same as the fluorescein concentration, which was determined using an extinction coefficient of  $77,000 \text{ M}^{-1} \text{ cm}^{-1}$  at 496 nm at pH 8.5 (Takashi *et al.*, 1979), because the fluorescein absorbance is pH dependent.

### Fluorescence anisotropy peptide binding assay

Peptide binding assays were set up and allowed to equilibrate for several hours. The binding of F-APPY (20–35 nM) to DnaK was found to be slow (on the order of multiple hours at submicromolar concentrations) requiring at least five hours to equilibrate at  $24^\circ\text{C}$ ; overnight equilibration at  $4^\circ\text{C}$  gave identical binding curves. Fluorescence measurements were made on an Alpha Scan Fluorometer (Photon Technology International) at  $24^\circ\text{C}$  with excitation at 492 nm, emission at 516 nm, and with 6 nm excitation, 6 nm emission slit widths. Experiments with added ATP (Figure 8) were performed under the same conditions; ATP was added just prior to measurement.

Since there was no observed intensity change in the fluorescein upon binding, the fraction of peptide F-APPY bound to DnaK at each point in the binding curve was calculated by the equation (Lakowicz, 1983):

$$\% \text{ F-APPY bound} = \frac{r - r_f}{r_b - r_f}$$

where  $r$  is the observed anisotropy of F-APPY at any point in the binding curve,  $r_f$  is the anisotropy of free F-APPY (determined at zero [DnaK]), and  $r_b$  is the anisotropy of DnaK bound F-APPY (determined from the anisotropy value in the plateau region of the binding curve). The data were fit to a quadratic single site binding equation (Reinstein *et al.*, 1990), using the program Kaleidagraph (Abelbeck Software).

### ATPase activity

Steady-state ATPase measurements were performed using a colorimetric assay which enzymatically couples ADP production with NADH oxidation and also regen-

erates ATP (Norby, 1988). Reactions were monitored over time at 340 nm by a Hewlett Packard 8452A Diode Array Spectrophotometer. Steady-state experiments were performed in 40 mM Hepes-KOH, 50 mM KCl, 11 mM Mg(OAc)<sub>2</sub> (pH 7.6), with 1 μM DnaK, 330 μM ATP at 30 °C for 15 minutes. Background hydrolysis was subtracted from each assay. The slope of the reaction (initial reaction rate) was determined by linear regression and divided by the DnaK concentration to determine the turnover number. DnaJ and GrpE stimulated steady-state ATPase measurements were made in the same fashion, and included 1 μM each of DnaJ and GrpE (generously provided by R. Russell and R. McMacken). Peptide stimulated steady-state ATPase measurements were similarly performed. The peptide NRW4 (NRLWLGTG) was synthesized by standard solid phase methods using F-Moc chemistry on a 9050 Plus PepSynthesizer (Millipore). The peptide molecular mass was confirmed by mass spectrometry. NRW4 was purified from minor contaminants on a C-18 reverse-phase column (Vydac). The extinction coefficient in water for NRW4 as determined by quantitative amino acid analysis (Molecular and Cellular Biology Protein Chemistry Core Facility, U. Mass., Amherst) was found to be  $\epsilon_{280} = 4.68 \times 10^3 \text{ M}^{-1} \text{ cm}^{-1}$ .

Single-turnover ATPase experiments were as described (Karzai & McMacken, 1996). Briefly, the ATPase reaction mixture contained 2.3 μM DnaK and  $\leq 30 \text{ nM } [\alpha\text{-}^{32}\text{P}]\text{ATP}$ , 3000 Ci mmol<sup>-1</sup> (ICN), in ATPase buffer with 5 mM DTT at 24 °C. Samples (15 μl) were removed at various times and quenched by the addition of 2 μl of 1 M HCl. A small portion (1-4 μl) of each quenched reaction was spotted on a thin-layer chromatography plate of PEI (polyethyleneimine) cellulose (EM Science). The plate was developed in a 1:1 (v/v) mixture of 1 M formic acid and 1 M LiCl. The data were quantified by PhosphorImager analysis (Molecular Dynamics). Hydrolysis in the absence of added DnaK ( $\leq 1.5\%$ ) was routinely subtracted from the data. The data were fit using a non-linear least squares algorithm in Kaleidagraph (Abelbeck Software) to a single exponential rate equation of the form:

$$\% \text{ ATP hydrolyzed} = H_f(1 - \exp(-k_1t))$$

where  $H_f$  is the asymptotic hydrolysis end point,  $k_1$  is the first-order rate constant, and  $t$  is the time in minutes. Data which were not well described by a single exponential fit were fit by a double exponential rate equation of the form:

$$\begin{aligned} \% \text{ ATP hydrolyzed} \\ = H_f - (A_1 \exp(-k_1t)) - [(H_f - A_1)(\exp(-k_2t))] \end{aligned}$$

where  $A_1$  is the amplitude of the first exponential process and  $k_2$  is the rate constant for the second exponential process.

$K_m$  and  $V_{max}$  measurements were performed using the enzymatic colorimetric ATPase assay (Norby, 1988). The K414I protein concentration was 1 μM in ATPase buffer with ATP concentrations between 0.047 μM and 39 μM. Results were plotted using the double reciprocal Lineweaver-Burke plot.

### Tryptophan fluorescence

Measurements of the ATP-induced blue shift of W102 were made in an Alpha Scan Fluorometer (Photon Technology International) with excitation at 295 nm, emission at 305-400 nm, and with 2 nm excitation slit width, 6 nm

emission slit width. Fluorescence spectra were measured in HMK buffer with 4 μM protein  $\pm$  0.48 mM ATP at 24 °C. The optical density of 0.48 mM ATP at 294 nm is 0.014, which is below the absorbance level ( $\geq 0.05$ ) which gives rise to decreased fluorescence due to the inner filter effect (Lakowicz, 1983).

### Hydrogen bonds in peptide binding domain of DnaK

Hydrogen bonds were identified using Insight II (Biosym Technologies Inc.) based on the atomic coordinates PDB 1DKX as described by Zhu *et al.* (1996).

### Acknowledgments

The authors thank Hwa-Ping Feng and Joanna Feltham for helpful discussions and critical readings of the manuscript; Huiara Chung for her preliminary work on the project; Roger McMacken for advice, suggestions, and co-chaperone proteins; Robert and Ruby McDonald for the use of their Alpha Scan Fluorometer; Jonathan Widom for the use of his reverse-phase HPLC system; Linda Rotondi for synthesizing peptide NRW4; and Robert Weis for the use of his DSC. This work was supported by a National Research Service Award GM16719 (D.L.M.) and grants GM38109 (R.I.M.) and GM27616 (L.M.G.) from the National Institutes of Health.

### References

- Alfano, C. & McMacken, R. (1989a). Ordered assembly of nucleoprotein structures at the bacteriophage  $\lambda$  replication origin during the initiation of DNA replication. *J. Biol. Chem.* **264**, 10699-10708.
- Alfano, C. & McMacken, R. (1989b). Heat shock protein-mediated disassembly of nucleoprotein structures is required for the initiation of bacteriophage  $\lambda$  DNA replication. *J. Biol. Chem.* **264**, 10709-10718.
- Banecki, B., Zyllicz, M., Bertoli, E. & Tanfani, F. (1992). Structural and functional relationships in DnaK and DnaK756 heat-shock proteins from *Escherichia coli*. *J. Biol. Chem.* **267**, 25051-25058.
- Beckmann, R. P., Mizzen, L. A. & Welch, W. J. (1990). Interaction of Hsp70 with newly synthesized proteins: implications for protein folding and assembly. *Science*, **248**, 850-854.
- Braell, W. A., Schlossman, D. M., Schmid, S. L. & Rothman, J. E. (1984). Dissociation of clathrin coats coupled to the hydrolysis of ATP: role of an uncoating ATPase. *J. Cell. Biol.* **99**, 734-741.
- Brodsky, J. L. (1996). Post-translational protein translocation: not all hsc70s are created equal. *Trends Biochem. Sci.* **21**, 122-126.
- Buchberger, A., Valencia, A., McMacken, R., Sander, C. & Bukau, B. (1994a). The chaperone function of DnaK requires the coupling of ATPase activity with substrate binding through residue E171. *EMBO J.* **13**, 1687-1695.
- Buchberger, A., Schröder, H., Büttner, M., Valencia, A. & Bukau, B. (1994b). A conserved loop in the ATPase domain of the DnaK chaperone is essential for stable binding of GrpE. *Nature Struct. Biol.* **1**, 95-101.
- Buchberger, A., Theyssen, H., Schröder, H., McCarty, J. S., Virgallita, G., Milkereit, P., Reinstein, J. & Bukau, B. (1995). Nucleotide-induced conformation-

- al changes in the ATPase and substrate binding domains of the DnaK chaperone provide evidence for interdomain communication. *J. Biol. Chem.* **270**, 16903-16910.
- Bukau, B. & Walker, G. C. (1990). Mutations altering heat shock specific subunit of RNA polymerase suppress major cellular defects of *E. coli* mutants lacking the DnaK chaperone. *EMBO J.* **9**, 4027-4036.
- Burkholder, W. F., Zhao, X., Zhu, X., Hendrickson, W. A., Gragerov, A. & Gottesman, M. E. (1996). Mutations in the C-terminal fragment of DnaK affecting peptide binding. *Proc. Natl Acad. Sci. USA*, **93**, 10632-10637.
- Cadwell, R. C. & Joyce, G. F. (1994). Mutagenic PCR. In *PCR Methods and Applications, Manual Supplement*, pp. 136-140, Cold Spring Harbor Laboratory Press, Cold Spring Harbor, NY.
- Chappell, T. G., Welch, W. J., Schlossman, D. M., Palter, K. B., Schlesinger, M. J. & Rothman, J. E. (1986). Uncoating ATPase is a member of the 70 kilodalton family of stress proteins. *Cell*, **45**, 3-13.
- Chappell, T. G., Konforti, B. B., Schmid, S. L. & Rothman, J. E. (1987). The ATPase core of a clathrin uncoating protein. *J. Biol. Chem.* **262**, 746-751.
- Creighton, T. E. (1993). Chemical properties of polypeptides. In *Proteins: Structures and Molecular Properties*, pp. 1-48, W. H. Freeman and Company, New York.
- Dodson, M., McMacken, R. & Echols, H. (1989). Specialized nucleoprotein structures at the origin of replication of bacteriophage  $\lambda$ . *J. Biol. Chem.* **264**, 10719-10725.
- Flaherty, K. M., DeLuca-Flaherty, C. & McKay, D. B. (1990). Three-dimensional structure of the ATPase fragment of a 70 K heat-shock cognate protein. *Nature*, **346**, 623-628.
- Flynn, G. C., Chappell, T. G. & Rothman, J. E. (1989). Peptide binding and release by proteins implicated as catalysts of protein assembly. *Science*, **245**, 385-390.
- Freeman, B. C. & Morimoto, R. I. (1996). The human cytosolic molecular chaperones hsp90, hsp70 (hsc70) and hdj-1 have distinct roles in recognition of a non-native protein and protein refolding. *EMBO J.* **15**, 2969-2979.
- Freeman, B. C., Myers, M. P., Schumacher, R. & Morimoto, R. I. (1995). Identification of a regulatory motif in Hsp70 that affects ATPase activity, substrate binding and interaction with HDJ-1. *EMBO J.* **14**, 2281-2292.
- Georgopoulos, C., Ang, D., Liberek, K. & Zylicz, M. (1990). Properties of the *Escherichia coli* heat shock proteins and their role in bacteriophage  $\lambda$  growth. In *Stress Proteins in Biology and Medicine* (Morimoto, R. I., Tissieres, A. & Georgopoulos, C., eds), pp. 191-221, Cold Spring Harbor Laboratory Press, Cold Spring Harbor, NY.
- Gragerov, A., Zeng, L., Zhao, X., Burkholder, W. & Gottesman, M. E. (1994). Specificity of DnaK-peptide binding. *J. Mol. Biol.* **235**, 848-854.
- Ha, J.-H., Hellman, U., Johnson, E. R., Li, L., McKay, D. B., Sousa, M. C., Takeda, S., Wernstedt, C. & Wilbanks, S. M. (1997). Destabilization of peptide binding and interdomain communication by an E543 K mutation in the bovine 70-kDa heat shock cognate protein, a molecular chaperone. *J. Biol. Chem.* **272**, 27796-27803.
- Harrison, C. J., Hayer-Hartl, M., Di Liberto, M., Hartl, F.-U. & Kuriyan, J. (1997). Crystal structure of the nucleotide exchange factor GrpE bound to the ATPase domain of the molecular chaperone DnaK. *Science*, **276**, 431-435.
- Hartl, F. U. (1996). Molecular chaperones in cellular protein folding. *Nature*, **381**, 571-580.
- Jordan, R. & McMacken, R. (1995). Modulation of the ATPase activity of the molecular chaperone DnaK by peptides and the DnaJ and GrpE heat shock proteins. *J. Biol. Chem.* **270**, 4563-4569.
- Kamath-Loeb, A. S., Lu, C. Z., Suh, W.-C., Lonetto, M. A. & Gross, C. A. (1995). Analysis of three DnaK mutant proteins suggests that progression through the ATPase cycle requires conformational changes. *J. Biol. Chem.* **270**, 30051-30059.
- Kang, P. J., Ostermann, J., Shilling, J., Neupert, W., Craig, E. A. & Pfanner, N. (1990). Requirement for hsp70 in the mitochondrial matrix for translocation and folding of precursor proteins. *Nature*, **348**, 137-143.
- Karzai, A. W. & McMacken, R. (1996). A bipartite signaling mechanism involved in DnaJ-mediated activation of the *Escherichia coli* DnaK protein. *J. Biol. Chem.* **271**, 11236-11246.
- Kraulis, P. J. (1991). MOLSCRIPT: a program to produce both detailed and schematic plots of protein structures. *J. Appl. Crystallog.* **24**, 946-950.
- Lakowicz, J. R. (1983). Fluorescence polarization. In *Principles of Fluorescence Spectroscopy*, pp. 111-153, Plenum Press, New York.
- Landry, S. J., Jordan, R., McMacken, R. & Gierasch, L. M. (1992). Different conformations for the same polypeptide bound to chaperones DnaK and GroEL. *Nature*, **355**, 455-457.
- Langer, T., Lu, C., Echols, H., Flanagan, J., Hayer, M. K. & Hartl, F. U. (1992). Successive action of DnaK, DnaJ and GroEL along the pathway of chaperone-mediated protein folding. *Nature*, **356**, 683-689.
- Liberek, K., Georgopoulos, C. & Zylicz, M. (1988). Role of the *Escherichia coli* DnaK and DnaJ heat shock proteins in the initiation of bacteriophage  $\lambda$  DNA replication. *Proc. Natl Acad. Sci. USA*, **85**, 6632-6636.
- Liberek, K., Marszalek, J., Ang, D., Georgopoulos, C. & Zylicz, M. (1991a). *Escherichia coli* DnaJ and GrpE heat shock proteins jointly stimulate ATPase activity of DnaK. *Proc. Natl Acad. Sci. USA*, **88**, 2874-2878.
- Liberek, K., Skowrya, D., Zylicz, M., Johnson, C. & Georgopoulos, C. (1991b). The *Escherichia coli* DnaK chaperone, the 70-kDa heat shock protein eukaryotic equivalent, changes conformation upon ATP hydrolysis, thus triggering its dissociation from a bound target protein. *J. Biol. Chem.* **266**, 14491-14496.
- McCarty, J. S., Buchberger, A., Reinstein, J. & Bukau, B. (1995). The role of ATP in the functional cycle of the DnaK chaperone system. *J. Mol. Biol.* **249**, 126-137.
- Mensa-Wilmot, K., Seaby, R., Alfano, C., Wold, M. S., Gomes, B. & McMacken, R. (1989). Reconstitution of a nine-protein system that initiates bacteriophage  $\lambda$  DNA replication. *J. Biol. Chem.* **264**, 2853-2861.
- Milarski, K. L. & Morimoto, R. I. (1989). Mutational analysis of the human HSP70 protein: distinct domains for nucleolar localization and adenosine triphosphate binding. *J. Cell. Biol.* **109**, 1947-1962.
- Miyazaki, T., Tanaka, S., Fujita, H. & Itikawa, H. (1992). DNA sequence analysis of the *dnaK* gene of *Escherichia coli* B and of two *dnaK* genes carrying the temperature-sensitive mutations *dnaK7* (Ts) and *dnaK756* (Ts). *J. Bacteriol.* **174**, 3715-3722.

- Montgomery, D., Jordan, R., McMacken, R. & Freire, E. (1993). Thermodynamic and structural analysis of the folding/unfolding transitions of the *Escherichia coli* molecular chaperone DnaK. *J. Mol. Biol.* **232**, 680-692.
- Nelson, R. J., Ziegelhoffer, T., Nicolet, C., Werner-Washburne, M. & Craig, E. A. (1992). The translation machinery and 70 kd heat shock protein cooperate in protein synthesis. *Cell*, **71**, 97-105.
- Norby, J. G. (1988). Coupled assay of Na<sup>+</sup>, K<sup>+</sup>-ATPase activity. *Methods Enzymol.* **156**, 116-119.
- Packschies, L., Theyssen, H., Buchberger, A., Bukau, B., Goody, R. S. & Reinstein, J. (1997). GrpE accelerates nucleotide exchange of the molecular chaperone DnaK with an associative displacement mechanism. *Biochemistry*, **36**, 3417-3422.
- Palleros, D. R., Welch, W. J. & Fink, A. L. (1991). Interaction of hsp70 with unfolded proteins: effects of temperature and nucleotides on the kinetics of binding. *Proc. Natl Acad. Sci. USA*, **88**, 5719-5723.
- Palleros, D. R., Reid, K. L., McCarty, J. S., Walker, G. C. & Fink, A. L. (1992). DnaK, hsp73, and their molten globules. *J. Biol. Chem.* **267**, 5279-5285.
- Pelham, H. R. B. (1986). Speculations on the functions of the major heat shock and glucose-regulated proteins. *Cell*, **46**, 959-961.
- Privalov, P. L. (1982). Stability of proteins: proteins which do not present a single cooperative system. *Advan. Protein Chem.* **35**, 1-104.
- Reinstein, J., Vetter, I. R., Schlichting, I., Rösch, P., Wittinghofer, A. & Goody, R. S. (1990). Fluorescence and NMR investigations on the ligand binding properties of adenylate kinases. *Biochemistry*, **29**, 7440-7450.
- Rüdiger, S., Buchberger, A. & Bukau, B. (1997a). Interaction of Hsp70 chaperones with substrates. *Nature Struct. Biol.* **4**, 342-349.
- Rüdiger, J. S., Germeroth, L., Schneider-Mergener, J. & Bukau, B. (1997b). Substrate specificity of the DnaK chaperone determined by screening cellulose-bound peptide libraries. *EMBO J.* **16**, 1501-1507.
- Sadis, S. & Hightower, L. E. (1992). Unfolded proteins stimulate molecular chaperone hsc70 ATPase by accelerating ADP/ATP exchange. *Biochemistry*, **31**, 9406-9412.
- Sambrook, J., Fritsch, E. F. & Maniatis, T. (1989). *Molecular Cloning: A Laboratory Manual*, Cold Spring Harbor Laboratory Press, Cold Spring Harbor, NY.
- Schmid, D., Baici, A., Gehring, H. & Christen, P. (1994). Kinetics of molecular chaperone action. *Science*, **263**, 971-973.
- Schönfeld, H.-J., Schmidt, D., Schröder, H. & Bukau, B. (1995). The DnaK chaperone system of *Escherichia coli*: quaternary structures and interactions of the DnaK and GrpE components. *J. Biol. Chem.* **270**, 2183-2189.
- Schröder, H., Langer, T., Hartl, F.-U. & Bukau, B. (1993). DnaK, DnaJ, and GrpE form a cellular chaperone machinery capable of repairing heat-induced protein damage. *EMBO J.* **12**, 4137-4144.
- Straus, D. B., Walter, W. A. & Gross, C. A. (1988). *Escherichia coli* heat shock gene mutants are defective in proteolysis. *Genes Dev.* **2**, 1851-1858.
- Szabo, A., Langer, T., Schröder, H., Flanagan, J., Bukau, B. & Hartl, F.-U. (1994). The ATP hydrolysis-dependent reaction cycle of the *Escherichia coli* Hsp70 system-DnaK, DnaJ, and GrpE. *Proc. Natl Acad. Sci. USA*, **91**, 10345-10349.
- Takashi, R. (1979). Fluorescence energy transfer between subfragment-1 and actin points in the rigor complex of actosubfragment-1. *Biochemistry*, **18**, 5164-5169.
- Theyssen, H., Schuster, H.-P., Packschies, L., Bukau, B. & Reinstein, J. (1996). The second step of ATP binding to DnaK induces peptide release. *J. Mol. Biol.* **263**, 657-670.
- Tilly, K., McKittrick, N., Zylicz, M. & Georgopoulos, C. (1983). The *dnaK* protein modulates the heat-shock response of *Escherichia coli*. *Cell*, **34**, 641-646.
- Wang, H., Kurochkin, A. V., Pang, Y., Hu, W., Flynn, G. C. & Zuiderweg, E. R. P. (1998). NMR solution structure of the 21 kDa chaperone protein DnaK substrate binding domain: a preview of chaperone-protein interaction. *Biochemistry*, **37**, 7929-7940.
- Wang, T.-F., Chang, J. & Wang, C. (1993). Identification of the peptide binding domain of hsc70. *J. Biol. Chem.* **268**, 26049-26051.
- Wawrzynów, A., Banecki, B., Wall, D., Liberek, K., Georgopoulos, C. & Zylicz, M. (1995). ATP hydrolysis is required for the DnaJ-dependent activation of DnaK chaperone for binding to both native and denatured protein substrates. *J. Biol. Chem.* **270**, 19307-19311.
- Wild, J., Kamath-Loeb, A., Ziegelhoffer, E., Lonetto, M., Kawasaki, Y. & Gross, C. A. (1992). Partial loss of function mutations in DnaK, the *Escherichia coli* homologue of the 70-kDa heat shock proteins, affect highly conserved amino acids implicated in ATP binding and hydrolysis. *Proc. Natl Acad. Sci. USA*, **89**, 7139-7143.
- Wu, B., Wawrzynów, A., Zylicz, M. & Georgopoulos, C. (1996). Structure-function analysis of the *Escherichia coli* GrpE heat shock protein. *EMBO J.* **15**, 4806-4816.
- Zhu, X., Zhao, X., Burkholder, W. F., Gragerov, A., Ogata, C. M., Gottesman, M. E. & Hendrickson, W. A. (1996). Structural analysis of substrate binding by the molecular chaperone DnaK. *Science*, **272**, 1606-1614.
- Zylicz, M., Ang, D., Liberek, K. & Georgopoulos, C. (1989). Initiation of  $\lambda$  DNA replication with purified host- and bacteriophage-encoded proteins: the role of *dnaK*, *dnaJ* and *grpE* heat shock proteins. *EMBO J.* **8**, 1601-1608.

Edited by M. Gottesman

(Received 18 September 1998; received in revised form 7 December 1998; accepted 14 December 1998)